Developing low cost and non-animal derived dynamic hydrogels for tissue engineering

Angela María Ramírez Rosales

MSc by Research

University of York

Department of Chemistry

June 2023

Abstract

Biomedical research needs to evolve towards more sustainable models by adopting the concept of the three Rs (reduction, refinement, replacement of animals in research). Additionally, economic limitations in emerging countries should also be taken into consideration. This project aims to develop a non-animal sourced and low-cost biomaterial that can be used to create accurate tissue models. We have developed a novel alginate-derived hydrogel, cross-linked with oxime bonds, by the synthesis of alginate derivatives: alginate-aldehyde and alginate-alkoxyamine. These dynamic covalent linkages lead to the formation of mechanically robust and stable hydrogel structures with self-healing properties. These properties mimic natural characteristics of some human extracellular matrices. Our long-term goal is to further functionalize with bioactive ligands also using oxime bonds. The output of this work will provide a platform from which to develop *in vitro* tissue models, based on affordable and renewable starting materials, suitable for the expansion of biomedical research in developing countries.

List of Contents

Abstract ***1***

List of Contents ***2***

List of Figures ***4***

Acknowledgements ***8***

Author's Declaration ***9***

Word Abbreviations ***10***

1. Introduction ***12***

1.1 Context and Motivation 12

1.1.1 Animal Studies 12
1.1.2 Economic discrimination 15

1.2 Proposal 16

1.3 Background 16

1.3.1 Human Soft Tissue 16
1.3.2 Hydrogels 17
1.3.3 Alginate 20
1.3.4 Dynamic Bonds 23

1.4 Aims & Objectives 24

2. Results and Discussion ***26***

2.1 Synthesis of Alginate Derivatives 27

2.1.1 Alginate Aldehyde (alg-ald) 2 27
2.1.2 Reproducing Alginate Alkoxyamine (alg-AA) 7 developed in the Roh Group[34] 29
2.1.3 Development of a novel route to access an Alginate Alkoxyamine (alg-AA) 3 31

2.2 Alginate Hydrogels 40

2.2.1 Ionically Crosslinked Alginate Hydrogels 40
2.2.2 Novel Oxime Crosslinked Alginate Hydrogels 46

2.3 Economic Analysis and Commentary 50

3. Conclusions and Future Work ***52***

4. Experimental ***55***

4.1 General Considerations 55

4.1.1 Synthesis of Alginate Derivatives 55
4.1.2 Alginate Hydrogels 56
4.1.3 Economic Analysis and Commentary 57

4.2 Synthesis of Alginate Derivatives 57

4.2.1 Alginate Aldehyde (alg-ald) 2 57
4.2.2 Reproducing Alginate Alkoxyamine (alg-AA) 7 developed in the Roh Group[34] 59
4.2.3 Development of a novel route to access an Alginate Alkoxyamine (alg-AA) 3 61

4.3 Alginate Hydrogels 70

4.3.1 Ionically Crosslinked Alginate Hydrogels 70
4.3.2 Novel Oxime Crosslinked Alginate Hydrogels 74

5. References 78

List of Figures

Fig. 1. A. Collagen and elastin fibers that compose the extracellular matrix (ECM). **B.** Native cells in the ECM.....17

Fig. 2. A. Polymer chains. **B.** Crosslinking of polymer networks with hydrophilic sites. **C.** Hydrogel formed when water is added and retained and the structure is swollen.....18

Fig. 3. Hydrogel with an ECM structure and native cells.....19

Fig. 4. The structure of the alginate molecule with its two monomers. **A.** Sodium Alginate, a common alginate salt **B.** Alginic Acid. **C.** "Egg-box" model of alginate chains in red crosslinked ionically by divalent cations in blue.....20

Fig. 5. The mechanism of EDC-mediated and NHS amine coupling in alginate.....22

Fig. 6. The mechanism of oxidation of alginate using Sodium metaperiodate.....22

Fig. 7. Reaction between an aminooxy group and an aldehyde to form an oxime bond..... 24

Fig. 8. Our approach of the oxime formation between alg-ald **2** and alg-AA **3**.....26

Fig. 9. Synthesis of Alginate Aldehyde.....27

Fig. 10. A. ^{1}H NMR Spectra of alginate and alg-ald (25%, 50% and 75% DOx). **B.** Closeup of the chemical shift range of interest, where the new peaks from the oxidation appear.....28

Fig. 11. DOSY Spectra of alginate and alg-ald (25%, 50% and 75% DOx).....28

Fig. 12. A. FT-IR Spectra of alginate and alg-ald **2** (25%, 50% and 75% DOx). **B.** Closeup of the FT-IR spectrum range of interest, where the aldehyde peaks appear.....29

Fig. 13. Synthesis of Sodium Alginate Alkoxyamine.....30

Fig. 14. A. ^{1}H NMR Spectra of alginate and the reproduced Alg-AA **X**. **B.** Closeup of a chemical shift range of interest, where the alkoxyamine are expected. **C.** Closeup of a chemical shift range of interest, where the new peaks of the Alg-AA are expected.....30

Fig. 15. Synthesis of the phthalimide protected amine.....32

Fig. 16. Scheme of the coupling alginate with the amine protected with the phthalimide group **12**, and the deprotection to form Alg-AA **3a**.....34

Fig. 17. A. ^{1}H NMR Spectra of alginate and the coupled alginate **12** at six different coupling ratios (darkest tone represents the highest coupling ratio of 2:5, descending to a lightest

hue representing the lowest coupling ratio of 1:96) compared to alginate. **B.** Closeup of a chemical shift range of interest, where the *phthal* peaks appear with intensities correlating to the coupling ratio.....34
Fig. 18. DOSY NMR Spectra of alginate and alg-AA-phthalimide **12** at 1:96 coupling ratio…35
Fig. 19. ^{1}H NMR Spectra of alginate, coupled alginate **12** (2:5 ratio), and deprotected alg-AA **3a**.....35
Fig. 20. Synthesis of the Boc protected amine.....36
Fig. 21. Scheme of the coupling alginate with the amine protected with the Boc group **15**, and the deprotection to form Alg-AA **3b**.....38
Fig. 22. ^{1}H NMR Spectra of alginate and coupled alginate **16** (2:5 ratio).....38
Fig. 23. DOSY NMR Spectra of alginate and coupled Alg-AA **16**.....39
Fig. 24. ^{1}H NMR Spectra of alginate, coupled alginate **16** (2:5 ratio), and deprotected alg-AA **3b** 39
Fig. 25. Organization of the plates. In the maroon coloured wells, alginate was added first and $CaSO_4$ was added next. In the dark wood-green coloured wells, the order of addition was the opposite. Hydrogels in columns 1-5 had a variation of ratios, and in the columns 8-12 the addition methods were varied. The arrow in column 10 represents the addition inside of the solution, and the spirals on columns 11-12 represent mixing motions.....41
Fig. 26. Ionically crosslinked alginate hydrogels. **A.** Hydrogels crosslinked at four different alginate to $CaSO_4$ ratios. Row A at 1:1, row B at 3:2, row C at 2:1 with the smallest hydrogels, and row D at 1:2 with the biggest hydrogels. **B.** Hydrogels with different addition methods. In rows A, B, the $CaSO_4$ solution was added on top of the alginate solution, whereas in rows C, D, the $CaSO_4$ solution was added first. In columns 8,9 the second solution was added on top, in 10, it was pipetted into the first solution, and in columns 11, 12, it was mixed.....42
Fig. 27. Ionically crosslinked alginate hydrogels. **A.** Hydrogel resulting from $CaCl_2$ added dropwise on top of alginate. **B.** Hydrogel resulting from $CaCl_2$ added to the side of the well with a slow and constant flow. **C.** Hydrogel resulting from $CaCl_2$ quickly added on top of alginate.....43

Fig. 28. Ionically crosslinked alginate hydrogels. **A.** $CaCl_2$ solution added on top of alginate. **B.** Alginate added after the calcium solution.....44
Fig. 29. Gelation problems in hollow moulds. **A, B.** Leaking. **C,D.** Fused hydrogels.....45
Fig. 30. Custom silicone moulds. **A.** Silicone mold making kit. **B.** Three step process: adding the silicone mixture (1A:1B mix ratio part A and Part B), using the negative to form the cylinder interior, the final mould.....46
Fig. 31. Scheme of the oxime crosslinked alginate hydrogels via alg-ald and novel alg-AA in DI H_2O.....47
Fig. 32. Two ionically crosslinked alginate hydrogels in DI H_2O.....47
Fig. 33. Oxime crosslinked alginate hydrogels via new alg-AA route and previously reported. First row (after 15 min): all the novel developed hydrogels (**A.**) were formed and the previously reported (**B.**) were in liquid solution. Second row (after 13 days): the novel developed hydrogels were still gelled, and only the previously reported formed in PBS gelled and the other were still liquid.....48
Fig. 34. Scheme of the oxime crosslinked alginate hydrogels via alg-ald and novel alg-AA in three different phosphate buffers: pH 6, PBS, pH 8.....49
Fig. 35. DOSY Spectra of alginate and alg-ald (25%, 50% and 75% DOx) **2**.....58
Fig.36. DOSY NMR Spectra of alginate and Na-alg-AA **12c** at 1:96 coupling ratio.....65
Fig. 37. DOSY NMR Spectra of alginate and coupled Alg-AA **16**.....69
Fig. 38. Organization of the plates. In the maroon coloured wells, alginate was added first and $CaSO_4$ was added next. In the dark wood-green coloured wells, the order of addition was the opposite. Hydrogels in columns 1-5 had a variation of ratios, and in the columns 8-12 the addition methods were varied. The arrow in column 10 represents the addition inside of the solution, and the spirals on columns 11-12 represent mixing motions.....71
Fig. 39. Types of addition of $CaCl_2$ solution on top of Alginate solution: **A.** dropwise, **B.** constant flow on the side, **C.** quickly added on top.....72
Fig. 40. Organization of the plates. In the maroon coloured wells, alginate was added first and $CaCl_2$ was added next. In the grey coloured wells, the order of addition was the

opposite. Rows A-C kept the alginate volume constant (150 µL), and rows E-G kept total volume constant (300 µL).....73
Fig. 41. Oxime crosslinked hydrogel preparation. **A**. Hydrogels prepared in custom made silicone moulds. **B**. Mechanism of the oxime crosslinking between the alginate-aldehyde **2** and the alginate-alkoxyamine **3b**.....75
Fig. 42. Elastic (G', in dark red) and viscous (G'', in light red) moduli of oxime crosslinked hydrogels (1% w/v at 1:1 ratio) in pH 6 buffer, with increasing shear strain (**A**) and frequency (**B**).....76
Fig. 43. Elastic (G', in dark green) and viscous (G'', in light green) moduli of oxime crosslinked hydrogels (1% w/v at 1:1 ratio) in PBS, with increasing shear strain (**A**) and frequency (**B**)…76
Fig. 44. Elastic (G', in dark purple) and viscous (G'', in light purple) moduli of oxime crosslinked hydrogels (1% w/v at 1:1 ratio) in pH 8 buffer, with increasing shear strain (**A**) and frequency (**B**).....77

Acknowledgements

Dr Chris Spicer is a bright and exemplary supervisor, he oriented me and taught me how the best quality of research comes from wellbeing, I am enormously grateful for his unhesitating help and support. Thank you for giving me the unique opportunity of joining your wonderful group and doing research in a project with high potential of positive impact. The biggest thanks for believing in me and inspiring me to believe in myself, my talents and my strengths. Thanks for encouraging me to achieve professional goals I thought unachievable. Thank you Dr Spicer for your guidance and for being the best supervisor.

I feel highly fortunate to have this nourishing experience at the University of York, the most welcoming and caring environment. I am full of gratitude to Dr Anthony H. Wild and the Wild Fund for your generosity, the Wild Platinum Scholarship and giving me this life-changing and fulfilling opportunity. Thanks to Rachel Crooks and the Chemistry Graduate Department for your humanity and offering the most integral programme. Very meaningful thanks to Yasmine Clarke at Open Door for your help when I needed it in the hardest moments.

Belonging to the Spicer Group was the highlight of the experience, a group where I felt genuine motivation, support, and collaboration. Thanks to my colleagues in the group, especially my mentor Laetitia Raynal, Nick Rose, Lydia Barber, and Reuben Breetveld. The people at E214 and Dr Iman Khazal, the MolMat and the Chemical Biology groups, especially Fraser Arnold and Dr Alfiya Suleymanova, from whom I learned a lot of chemistry and keep the best memories. Thanks to Prof David Smith for his guidance and asking questions that encouraged me with critical thinking. Thanks to all the technical staff, Heather Fish and Alex Heyam at NMR, Mark Roper at the mechanical workshop, Mike Keogh and Steve Hau at stores, and Karl Heaton at MS. Thanks to all the staff at the E building for their care and kindness, particularly Denisse and Debbie.

I could not have undertaken this journey without my mom and my dad, thanks for their most unlimited and authentic love and support, for always boosting me to reach my dreams and giving me the life tools to be who I am. My siblings for their help and for always giving me the wisest advice. Thanks Pixie for your unconditional emotional support. Thanks to Leo Durán and Deepika Kondral for becoming my family in the UK.

I feel grateful for being born in beautiful Colombia, where I found the inspiration to think outside the box, put my personal touch in the project and hopefully inspire others. Participating in this project gave me immense personal growth, confidence of working independently in the lab, preparation for my future professional aspirations I was initially looking for, and the best memories and friendships. Today, I am a better person thanks to this experience.

Muchas gracias.

Author's Declaration

I declare that this thesis is a presentation of original work and I am the sole author. This work has not previously been presented for an award at this, or any other, University. All sources are acknowledged as references.

Angela María Ramírez Rosales

Word Abbreviations

Alg	Alginate
Ald	Aldehyde
AA	Alkoxyamine
Ar	Argon gas
Boc	*Tert*-butoxycarbonyl
br	Broad
$CaCO_3$	Calcium carbonate
CbzCl	Benzyl chloroformate
$CDCl_3$	Deuterated chloroform
$CHCl_3$	Chloroform
d	Doublet
DBU	1,8-diazabicyclo(5.4.0)undec-7-ene
DCM	Dichloromethane
dd	Doublet of doublets
DEAD	Diethyl azodicarboxylate
DIAD	Diisopropyl azodicarboxylate
DI H_2O	Deionized water
DMSO	Dimethylsulfoxide
D_2O	Deuterated water
DOSY	Diffusion ordered spectroscopy
DOx	Degrees of oxidation
ECM	Extracellular matrix
EDC	1-Ethyl-3-(3-dimethylaminipropyl)carbodiimide
Et_3N	Triethylamine
Et_2O	Diethyl ether
EtOAc	Ethyl acetate
FT-IR	Fourier-transform infrared spectroscopy
h	Hours

m	Multiplet
M	Molar
MeOH	Methanol
$MgSO_4$	Anhydrous magnesium sulfate
MS (ESI)	Electrospray Ionization Mass Spectrometry
m/z	Mass to charge ratio
$NaIO_4$	Sodium metaperiodate
NaOH	Sodium hydroxide
Na_2SO_4	Anhydrous sodium sulfate
NHS	N-hydroxysuccinimide
PBS	Phosphate-buffered saline
Pd/C	Palladium on carbon
PPh_3	Triphenylphosphine
PTFE	Polytetrafluoroethylene
RGD	Arginylglycylaspartic acid
RT	Room temperature
s	Singlet
t	Triplet
TBA	Tetrabutylammonium
TBAF	Tetrabutylammonium fluoride
THF	Tetrahydrofuran
USD	United States Dollar

1. Introduction

1.1 Context and Motivation

1.1.1 Animal Studies

Animal testing is a topic that generates a lot of debate. Non-human animal (hereafter "animal") models are often used in biomedical research for *in vivo* testing of developed products that can represent a risk to humans. It is assumed that this is the best practice to identify if a possibly-hazardous-product is safe for human use.[1,2] Its purpose is to acquire toxicology data to understand a disease or tissue behaviour and responses to stimuli (e.g. foreign biomaterial being studied *in vivo*), ultimately to generate confidence in the use of the product in human trials. However, the methods used in animal studies are unsustainable and can be considered unethical.[3] Animal studies *can* sometimes have a positive impact in humans but this is balanced against considerable negative consequences: the potential to save human lives comes at the expense of the life and welfare of other animals. Alternatively, numerous deaths of both models and humans can be caused by misleading positive results in models that do not correlate to those obtained in human clinical trials.[4]

The harm-benefit analysis[4,5] of animal testing should be given major attention, due to the high levels of failure in preclinical trials and attrition in drugs discovery.[6-9] This especially occurs because animal testing results are unreliable and unpredictable.[6,8,10] There is a translational failure from animals to humans of more than 90%,[7,8,10-13] but the favourable <10% results do not correlate to those in human studies, since only 1 out of 10 of these approved tests is successful in human trials.[7,9,11,14] In other words, less than 1% of animal experiments represent a scientific advance that reaches the clinic. In 2005 in Europe, more than 6 million animal models were used in the pharmaceutical industry, and only 12 new substances were released (not taking into account drug withdrawal from the market).[15] This means that even if a drug has been labelled as "safe" in an animal model, during clinical trials it is most likely that it will fail or could even harm or kill humans.[10]

The results in animal models are poorly translatable to humans because of biological natural variation and physiological differences.[6,16] Modelling human physiology with non-human animals is like comparing pears and apples, there are specific shared similarities but each one represents a very different system. The initial planning and the selection of a particular model for an experiment is highly conditioned by having common anatomy and biological phenomenon,[1,2] but the type of animal model needed can even depend on the data and results yet to be obtained by the experiment being designed.[4,8] Due to the high levels of interspecies heterogeneity, assumptions and extrapolation of results from trials from one species to another is risky,[6] and may result in false negatives and false positives that can cause direct harm in humans[6,10] and significant economic losses. For example, a drug to treat Type 2 Diabetes called Mediator® was developed by the French pharmaceutical Servier, with results in animal models showing improved glucose tolerance and decreased insulin resistance. These studies had misleading preclinical results that when commercialized caused between 500-2000 human deaths from heart valve disease.[17,18,19] The company initially earned $2.7M through this medicine, but after the company was found guilty of deception and manslaughter, they had to compensate €180M in damages.[4] In other cases, drugs with therapeutic potential in humans are identified as "toxic" in animals, and instead of further development, these are discarded.[10] A simple example is the toxicity of avocado and chocolate in dogs:[20] if regulated by animal testing, these widely beloved foods with multiple nutritional benefits[21,22] would have been banned from human consumption. This emphasizes the imperative need to develop **accurate** human-relevant tissue models.

To address some of these *inhumane* issues, William M. S. Russell (zoologist and psychologist) and Rex L. Burch (microbiologist) wrote "The Principles of Humane Experimental Technique" (commonly known as "The Principles") in 1959, where they introduced the concept of the three Rs: Reduction, Refinement, Replacement.[3] In biomedical research, the three Rs translate into the *reduction* in the numbers of animals used, the *refinement* of the procedures applied in order to minimize animal suffering, and the *replacement* overall of animal models with procedures which do not use conscious living

vertebrates.[23] However, after more than 60 years since this book being published, the number of animals used in biomedical research has not fallen but even increased, some handling methods have improved but lab conditions have not, and replacement initiatives are not widely used.[4,24,25,26]

The UK is believed to have the strictest regulations on animal research.[27] However, since this is relative to other countries, it does not mean the regulation itself is strict. UK Animal Research regulation follows the Animals (Scientific Procedure) Act (ASPA) introduced in 1986.[5,27] This document restricted in many cases the use of living vertebrates, banning experimentation on some apes and the use of animal models in non-essential fields like cosmetics. Animal models can only be used when there are no alternatives and the expected results prevail over the negative consequences, for example, advancement in human healthcare. However, according to the Annual Statistics of Scientific Procedures on Living Animals Great Britain 2021,[24] more than 3 million scientific procedures involving living vertebrates were performed in 2021, 6% more than the previous year. Furthermore, in 2021 the number of procedures performed with animal models was the same as in 1986 when the ASPA was introduced, meaning the number of procedures with animals has not been decreasing after more than 30 years of the ASPA regulations, contrary to what was expected. Based on ASPA, these large number of animal models have not decreased because there is a need for the design and creation of more accurate *in vitro* models.[24]

In addition to the direct disadvantages of animal testing, another considerable drawback is the high costs of these experiments.[10] For example, the cost of a single carcinogenicity test in 2005 in Europe involving 400 animals, was more than €780,000, and the total annual cost was €82 M just for carcinogenicity studies,[15] which on average take between 5-10 years. Due to the attrition rates previously mentioned, the most likely outcome from these studies is translational failure, at a cost of more than £81 M, and in the unlikely case of a market release, an 8% chance of drug withdrawal in carcinogenicity[10] after commercialization would have increased the economic loss even more. The estimate of the global market for animal testing in 2018 was more than $80 billion US dollars,[10] and taking into account the

high translational failure, this depicts a broad economic leak in biomedical research. The costs of biomedical research and studies should be included in the reports to create awareness of the economic loss from inefficient areas such as animal testing, but also of the economic inequalities in the biomedical research field between countries.

Animal models have been used for more than two and a half millennia[28] and remain a common step in clinical trials today, despite the known limitations outlined above. Current cheaper and faster alternatives include *in silico* modelling with artificial intelligence, *in vitro* toxicology studies, and complex designs of organoids and organs-on-a-chip.[25] However, these solutions have not yet entirely replaced or accomplished the complete modelling of a human system. Moreover, although these alternatives can reduce the immense costs of animal testing, these are not economically inclusive with all types of biomedical research and tissue engineering in emerging countries around the world. Biomedical research is in urgent need of evolving towards more accurate and sustainable models that are safer for people.

1.1.2 Economic discrimination

Economic inequality in biomedical research among countries is a hidden or possibly ignored issue. A poorly-cited paper from *Nature* about discrimination in science[29] talks about critical topics like gender, age, ethnicity, disability and even religion, but the matter of economic discrimination is barely brought up. Although the budgetary limitations among labs from different countries was not taken into account in this article, it mentions how people from lower socioeconomic backgrounds face disadvantages, which can be extrapolated to labs located in underprivileged regions in the world also facing disadvantages. It also points out how people from these backgrounds feel motivated to study harder in order to fit in the capital-dependent system. According to Clarivate, more than 72% of the "Highly Cited Researchers" in 2022 come from only 5 developed countries: United States, China, United Kingdom, Germany, and Australia.[30] A study in the US about grant processes for biomedical research suggests that underrepresented minority groups are at a disadvantage during applications.[31] Higher diversity in a STEM workplace has shown to translate into gains,[32] but

the diversification of research in terms of high-quality and low-cost studies would translate into a growth in knowledge and increase the possibilities of answering the countless medical interrogations we still have nowadays.

1.2 Proposal

Taking into account the limitations of current biomedical research described above, a solution to animal testing and economic inequality is to develop a platform for *in vitro* tissue models of increasing complexity,[33] suitable to the expansion of biomedical research in emerging countries. In order to mimic a native soft human tissue, the material must have dynamic properties and a highly hydrated environment. But it should also be made from cheap and renewable starting materials. After fulfilling these conditions, when imitating a specific tissue it must ensure the desired interaction with the corresponding cells.

In this project, we developed new low-cost alginate-based hydrogels in which oxime bonds[34,35,36,37] are used as crosslinkers to give the material tunable self-healing properties.[38] Oxime bonds are expected to be used to functionalise the materials with biologically active motifs in future work to enable cell adhesion and control biochemical signalling.

1.3 Background

1.3.1 Human Soft Tissue

Human soft tissue is an unmineralized material where cells reside in an extracellular matrix (ECM), characterized by having high flexibility and soft mechanical properties.[39] This matrix is mainly composed of elastin and collagen (Fig. 1), a group of proteins that characterize connective tissues.[40] The environment of the ECM plays a key role in determining cell fate and function. [41]

Designing materials that mimic tissues within the human body and have direct interactions with cells is challenging due to the structural complexity, high variability and dynamic state of the ECM. It is crucial to understand key factors involved in native tissue growth, such as

the shape and size of cells,[42] genetics, biochemistry, physiology,[43] composition, porosity,[44] mechanical properties, viscoelasticity,[41] among many others.

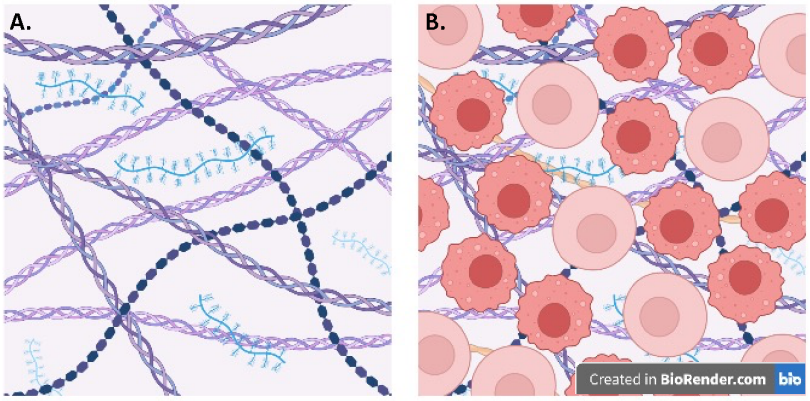

Fig. 1. A. Collagen and elastin fibers that compose the extracellular matrix (ECM).

B. Native cells in the ECM.

1.3.2 Hydrogels

A gel is a "non-fluid [sol] colloidal network or polymer network that is expanded throughout its whole volume by a fluid" (UIPAC definition). In other words, it is a solution consisting of a dispersed non-fluid solid phase, often a polymer network or aggregate of particles, that increases its volume by absorbing and retaining a continuous liquid phase.[45,46] More specifically, a *hydro*-gel is a type of gel that is expanded by water (Fig. 2).[47] The chains or particles within a hydrogel can either be hydrophilic or a mixture of hydrophilic and hydrophobic components (Fig. 2.B), but the material must be able to favourably interact with water to remain expanded.[48] The mixed polymer(s) chains within gels undergo crosslinking, which forms a network that structures the gel and provides resistance to dissolution in the liquid phase (Fig. 2.A,B). These crosslinking events can occur between chains forming interpenetrating polymer networks.[48] The nature of the polymer(s) and crosslinking(s) define the material's properties which can be designed for a variety of applications like the food industry and healthcare.[46]

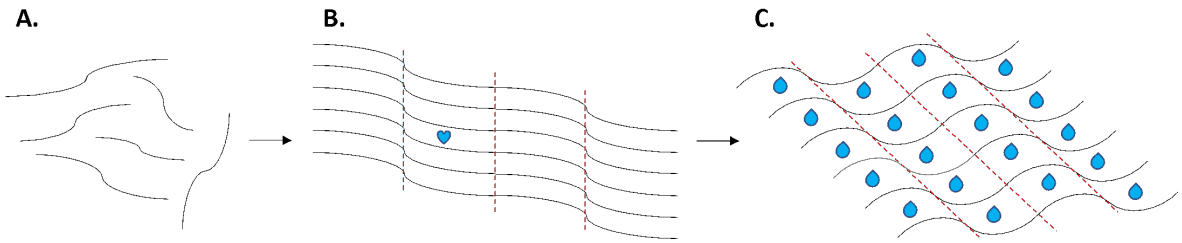

Fig. 2. A. Polymer chains. **B.** Crosslinking of polymer networks with hydrophilic sites. **C.** Hydrogel formed when water is added and retained and the structure is swollen.

Hydrogels can be classified according to the nature of their crosslinking: physical or chemical.[48,49] Physical crosslinking occurs when polymer chains entangle or are held together by non-covalent interactions (like ionic and hydrogen bonds or hydrophobic interactions) between the functional groups present in the chains. These non-covalent interactions result in gels with viscoelastic behaviour that can change in response to environmental conditions or factors such as temperature or pH, and crosslinking is often dynamic and reversible. On the other hand, chemical crosslinking relies on the formation of covalent bonds,[50] resulting in more mechanically resistant gels with elastic properties. The selection of the type of crosslinking has a major influence on the properties and applications of the hydrogels.

Within a hydrogel, the solid phase suspended in a liquid medium provides the material with both solid- and liquid-like behaviour.[41] The mechanical characteristics and the highly hydrated environment of a hydrogel imitate the properties of the natural soft tissues found in the human body;[41,48] especially since many human tissues are already considered natural hydrogels, like the vitreous humor in the eyes.[51,52] For instance, the high water content provides viscous damping to decrease deformation and allows the free diffusion of molecules facilitating the transport of oxygen and nutrients[50,51] simulating molecule diffusion in native ECM. Therefore, hydrogels are promising for biomedical industries and biomedical research areas like tissue engineering.[36,44,52,53]

Hydrogels have been widely used as bioinks and 3D structures for *in vitro* tissue models, as nanoparticles for drug delivery, and as scaffolding for wound healing and alternatives for organ transplants.[44,54] They can be designed with different and tunable mechanical, chemical and biological properties depending on the tissue and function to replicate. For example, the extracellular matrix (ECM) in connective tissue has a specific porosity[44] that enables cells like fibroblasts to attach and proliferate, which must be replicated when designing synthetic ECM (Fig. 3). Additionally, the ECM provides extracellular biological signals and growth factors that control the adhesion and behaviour of cells within the tissue[44,55,56], a design that can be replicated within a hydrogel. The right design depends on reproducing the right characteristics.

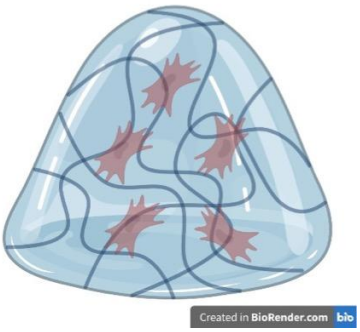

Fig. 3. Hydrogel with an ECM structure and native cells.

Furthermore, the properties of hydrogels depend on the polymer.[50,57] Natural polymers such as collagen, carrageenan and alginate often possess high biocompatibility but also suffer high batch to batch variation and are prone to contamination.[57,58,59,60] Alternatively, synthetic polymers like polyethyleneglycol have the advantages of having a designed structure and having defined characteristics and/or tunable properties like water absorption capacity, biodegradability and durability.[57,58,59] However, synthetic polymers tend to be bioinert and commonly induce immunological responses in the body. Sometimes this can be solved by the derivatization of biomaterials to improve their properties, for example, through the addition of cell adhesive peptides to bind cells and improve the bioactivity of a hydrogel.[50,55]

1.3.3 Alginate

In our project we chose to work with alginate hydrogels since these are a very common type of hydrogel used in tissue engineering. Alginate is an anionic polysaccharide found in the cell walls of brown algae,[61] which is a cheap, fast-growing and self-renewable source. It has linear copolymeric structure consisting of β-D-mannuronate (M-block or mannuronic acid) and α-L-guluronate (G-block or guluronic acid)[50,60,61,62,63] (Fig. 4.A,B). The G-blocks within an alginate chain have the capacity to bond with divalent cations, forming a cross-linked structure commonly referred to as the "egg-box" model due to its particular shape (Fig. 4.C) and inducing rapid hydrogelation in aqueous solutions.[50] Alginates have molecular weights of 20-600 kDa.[61]

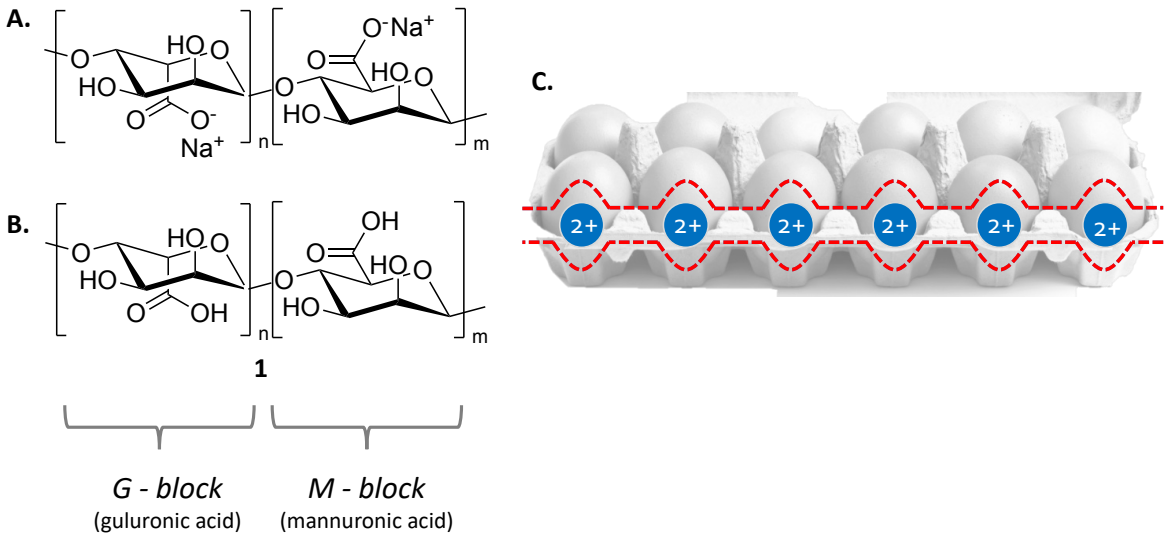

Fig. 4. The structure of the alginate molecule with its two monomers. **A.** Sodium Alginate, a common alginate salt **B.** Alginic Acid. **C.** "Egg-box" model of alginate chains in red crosslinked ionically by divalent cations in blue.

Alginate **1** is widely used in multiple fields due to its biocompatibility and gelling properties. For example, it is often used as a gelling agent in the food industry, in products like hot sauces, jams, and edible water beads, as well as in biomaterials for pharmaceutics,

healthcare and biomedical research.[36,61,64,65] It is an affordable and sustainable material with a wide range of applications.

Alginate can absorb 17-40 times its weight in water,[61-63,66] meaning it is superabsorbent and can form *hydrogels*. Divalent cations are often used to ionically crosslink alginate. Calcium sources like calcium(II) chloride, calcium(II) sulfate and calcium(II) carbonate,[50] are mainly used since these hydrogels have been proven to be biocompatible. However, other divalent cations can be used but may cause disruptions in the human physiology, such as strontium and zinc, which have osteogenic properties.[50] Another example is barium cations, which can form stronger gels but at high concentrations can block potassium channels. Even though other cations like copper and cadmium have high affinity for alginate and make stiffer gels, these are toxic in the human body and cannot be used for these purposes.[50]

Nevertheless, ionically crosslinked alginate hydrogels have certain disadvantages that limit their use. Collapse of the hydrogel when ions leak out is the main problem, limiting the durability of the gel.[67] This can be solved by using covalent crosslinking,[35] particularly dynamic reversible bonds that provide self-healing properties.[41,67] In both cases, alginate hydrogels are gelled via crosslinking reactions that occur from mixing two liquid components.[37]

Alginate is a molecule that can be easily modified in different ways on its carboxylic acid functional group.[1,2] For example, using coupling agents to introduce molecules into the structure, such as the coupling of an amine using EDC, which couples primary amines to carboxylic acids by forming an activated ester leaving group. EDC is often used with NHS (Fig. 5), a chemical modification reagent that activates carboxylates and increases the efficiency of EDC-mediated coupling.

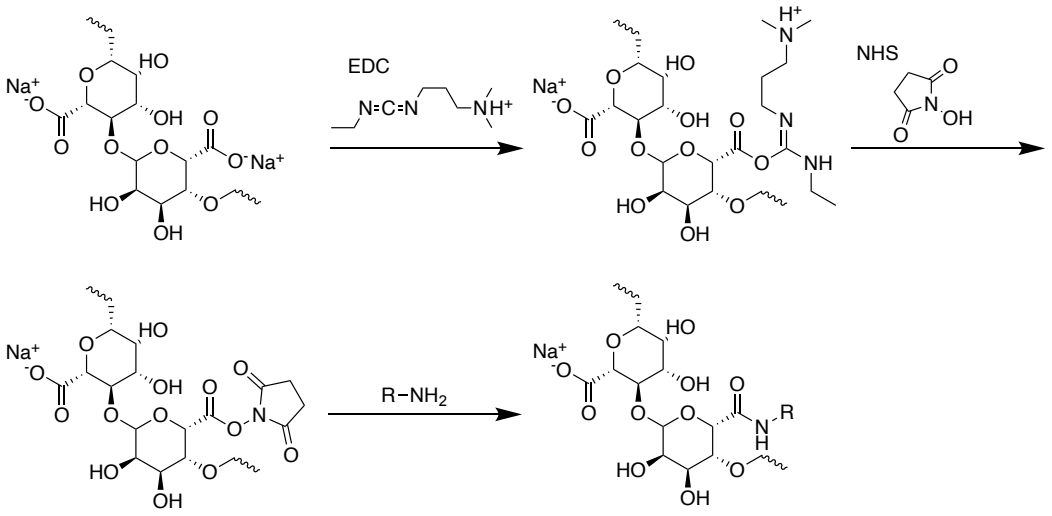

Fig. 5. The mechanism of EDC-mediated and NHS amine coupling in alginate.

Another way of modifying the molecule is by opening the ring via an oxidation.[36] Using an oxidising agent such as sodium metaperiodate, which cleavages the diols and opens the alginate chain to form two aldehydes (Fig. 6) at different degrees of oxidation.[34]

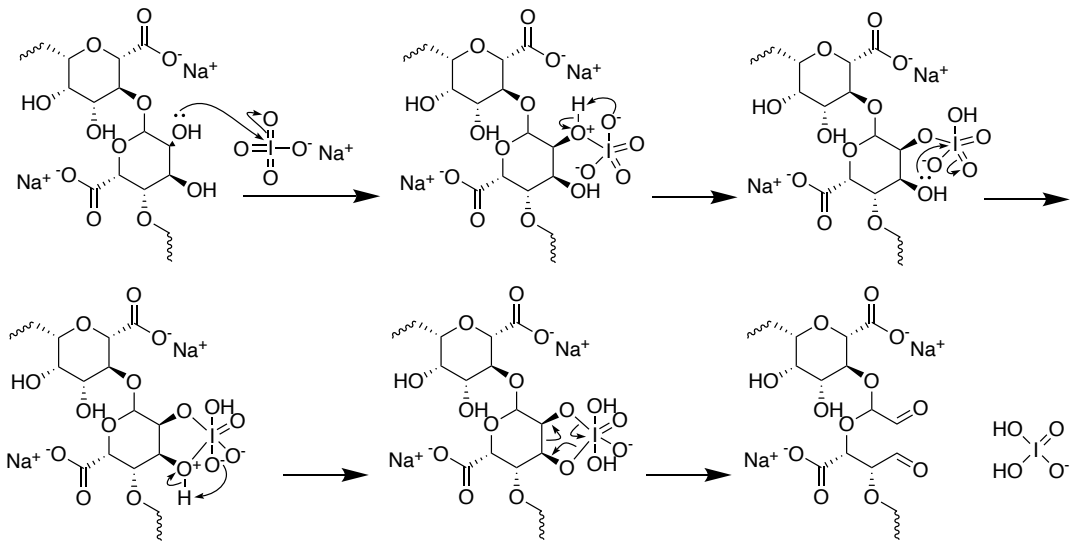

Fig. 6. The mechanism of oxidation of alginate using Sodium metaperiodate.

Although alginate is biocompatible, on its own, it is bioinert and cells cannot adhere to it.[34,50] In most cases, it is mixed with other polymers and materials with bioactive properties to address this limitation.[64] Alternatively, it is derivatized and functionalized with molecules that enable the interaction with human cells. One way to modify the alginate in order to mimic native ECM, is by functionalizing it at the carboxylic acid with cell adhesive peptides such as arginylglycylaspartic acid peptides (RGDs).[55] This represents a major limitation of alginate hydrogels to mimic all biological properties and environments, so these have not modelled a complete animal organism or replaced animal models to date.

In summary, we chose alginate because it is biocompatible, non-animal derived, low-cost, and its source (brown algae) is self-renewable.

1.3.4 Dynamic Bonds

To improve ionically crosslinked alginate hydrogels, we explored dynamic covalent bonds and their properties. Dynamic bonds are a type of covalent bond characterized by being equilibrium, meaning these reversible bonds can break and re-form under ambient conditions.[67] They are often responsive to different stimuli and conditions such as temperature and pH. Materials that are crosslinked via dynamic bonds can adapt and show self-healing and recycling properties.[35] Examples of dynamic bonds that have been used to form hydrogels are disulphide bonds, boronic ester formation, and imines.[41,68,69]

Employing dynamic bonds is useful in fields like biomaterials and tissue engineering.[41] Dynamic covalent materials can be modified and designed with tunable properties, which can allow the development of 3D networks that mimic native ECM.[70] For example, in tissue engineering, building a scaffold with the correct tunable mechanical and viscoelastic properties is key to properly imitate the extracellular matrix in a tissue. Also, the environmental conditions of the mimicked tissue, such as pH and temperature, must be considered for the design and gelation of the hydrogel scaffold.[41] Furthermore, a dynamic biomaterial allows a range of values for different characteristics from which very accurate and personalised models can be made by choosing each value accordingly to each patient.

However, some properties are highly interdependent, which has challenged these expectations of controlling properties of the biomaterials.[64]

Oximes are a type of imine that is formed by the reversible addition or exchange reactions[41] of an alkoxyamine and an aldehyde or ketone (Fig. 7).[73] The reaction is sensitive to pH, with oxime formation favoured at pH 4-6.[34] As with imines, oximes have self-healing properties,[67] and are degradable and can be used for 3D printing.[68,71] However, oximes are far more resistant to hydrolysis than imines, allowing the formation of more stable and mechanically strong hydrogels.[41,72]

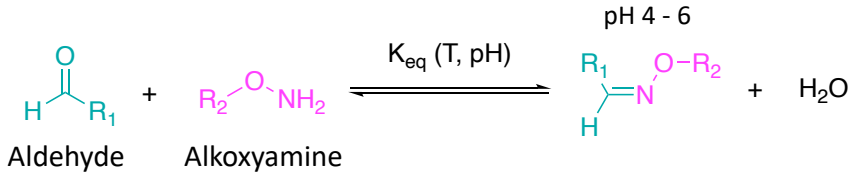

Fig. 7. Reaction between an aminooxy group and an aldehyde to form an oxime bond.

1.4 Aims & Objectives

To develop and study new oxime-crosslinked alginate hydrogels we need to:

✓ Synthesize and characterize three alginate derivatives: Alginate Aldehyde (alg-ald), and Alginate Alkoxyamine (alg-AA) via a previously reported route and a novel route.

✓ Prepare and compare alginate hydrogels: ionically-crosslinked, previously reported oxime-crosslinked alginate hydrogels, and the new oxime-crosslinked alginate hydrogels.

✓ Characterize the new oxime-crosslinked alginate hydrogels.

✓ Perform an economic analysis to evaluate the value of the new hydrogels.

In order to achieve our proposal and previous objectives, we followed three steps. First, we synthesized and characterized the alginate derivatives: alg-ald and alg-AA. Second, we prepared and studied ionically-crosslinked (control) and oxime-crosslinked alginate hydrogels by mixing solutions of the synthesized molecules, and characterized the new

hydrogels with oscillatory shear rheological experiments to measure their viscoelastic properties. Finally, we did a basic economic analysis from the costs of the reagents and solvents to understand the possibility of designing a low-cost material.

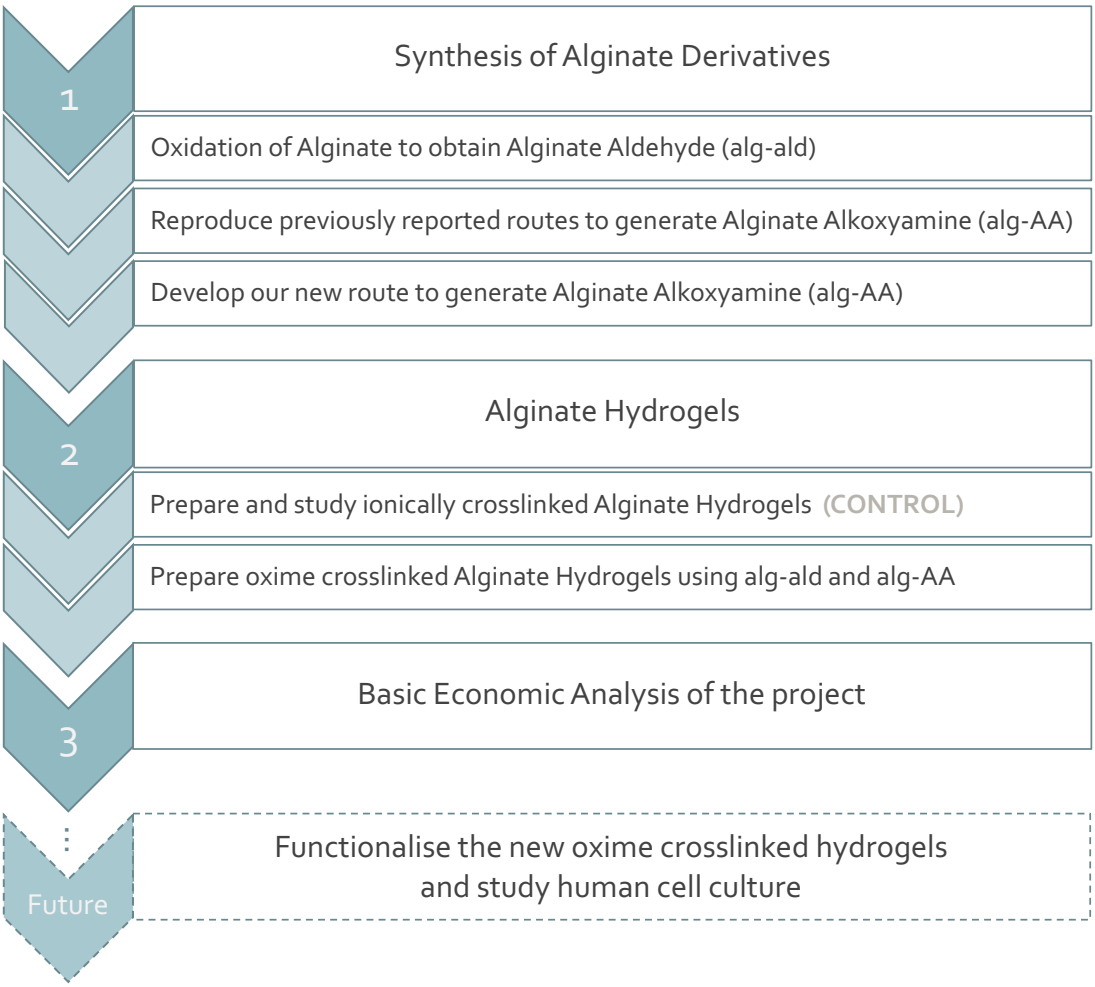

Future work consists in functionalizing the new oxime-crosslinked hydrogels with adhesive RGB peptides and study how this functionalisation supports the culture of human cells.

2. Results and Discussion

In order to achieve our goal of developing an affordable and sustainable platform for *in vitro* tissue models that mimics soft human tissue we decided to develop an enhanced alginate hydrogel. Alginate is a biocompatible material extracted from brown algae, a self-renewable source, which meets our sustainability goal. Hydrogels offer a highly-hydrated environment and the viscoelastic and chemical transport properties characteristic of native soft tissue.[50,51] However, as described earlier, alginate is typically gelled via ionic crosslinking, forming weak and unstable hydrogels. To design a hydrogel with dynamic properties, we decided to crosslink the alginate via a dynamic covalent linkage, the oxime bond.

Using the oxime bond to covalently crosslink alginate hydrogels could provide tunable mechanical properties. Oximes have been used previously to crosslink alginate hydrogels by introducing difunctional crosslinkers,[74,75] or by modifying the alginate to form polymers bearing either aldehyde or alkoxyamines (Fig. 8). The second method has been previously developed by the Roh group, where they modified the backbone of sodium alginate to introduce alkoxyamine and produced alginate-aldehyde to form oxime-crosslinked alginate hydrogels with tunable mechanical properties. However, we started by recreating these in our group but noticed these hydrogels faced various challenges in reproducibility. For this reason we developed new hydrogels (Fig.8) with an easier route to synthesize an alginate-alkoxyamine and compared these to the previously developed in the Roh Group.[34] This is outlined in the next section.

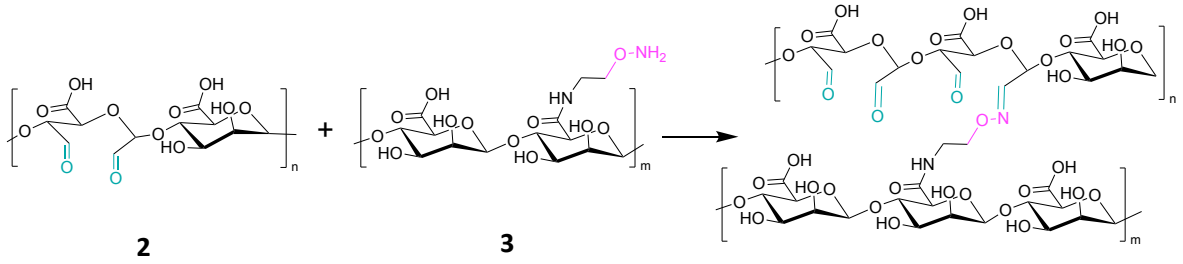

Fig. 8. Our approach of the oxime formation between alg-ald **2** and alg-AA **3**.

2.1 Synthesis of Alginate Derivatives

In our attempts to recreate the material produced by the Roh group, two molecules were synthesized. We reproduced the alginate aldehyde (alg-ald) and the alginate alkoxyamine,[34] but due to limitations in the route to synthesize an alg-AA, we synthesized alginate alkoxyamine (alg-AA) via a novel route and we compared it to the previously reported one.[34]

2.1.1 Alginate Aldehyde (alg-ald) 2

We prepared the alginate aldehyde **2** by oxidizing the sugar backbone at three different degrees of oxidation (25%, 50% and 75% DOx) using sodium metaperiodate ($NaIO_4$) as an oxidizing agent (Fig. 6, Fig. 9).[34] According to the protocol used and the reagents employed, the cost of the reagents to make 1 g of this Alg-ald with 50% DOx was approximately $24 USD.

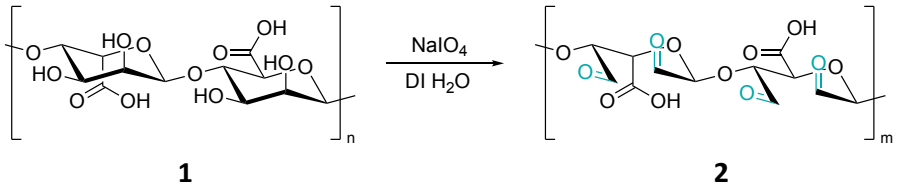

Fig. 9. Synthesis of Alginate Aldehyde.

The products **2** were purified by dialysis to remove excess reagents, and the lyophilised products characterized using ^{1}H NMR, Diffusion Ordered Spectroscopy NMR (DOSY NMR), Fourier-transform infrared spectroscopy (FT-IR).

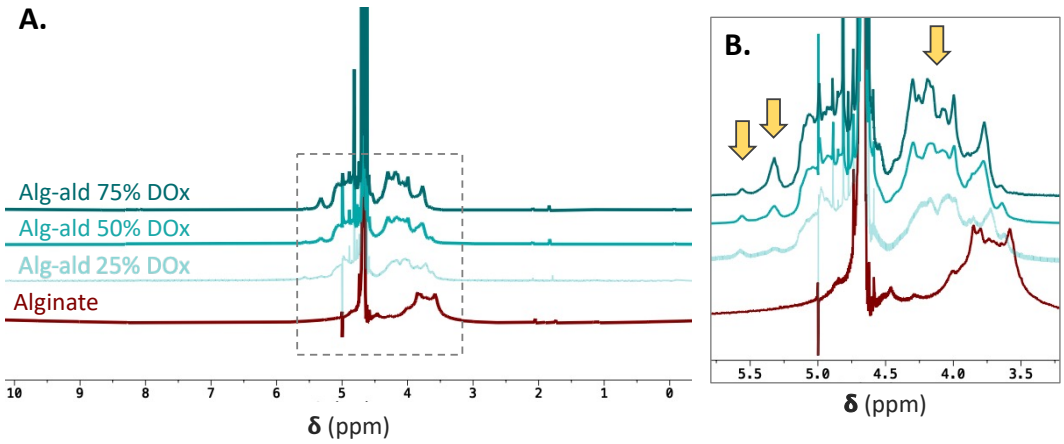

Fig. 10. A. ^{1}H NMR Spectra of alginate and alg-ald (25%, 50% and 75% DOx). **B.** Closeup of the chemical shift range of interest, where the new peaks from the oxidation appear.

The ^{1}H NMR spectra of alginate aldehyde at 25% DOx, 50% DOx, and 75% DOx compared to alginate (Fig. 10), revealed the appearance of peaks at 4.2 ppm, 5.3 ppm and 5.6 ppm, corresponding to the ring-opened sites of oxidation as reported in the literature.[76] The characteristic aldehyde peak (around 9 to 10 ppm) would not be seen because the experiment was made in D_2O. Additionally, the intensity of the peaks correlate with the degree of oxidation, and confirm the ability to tune and access different DOxs.

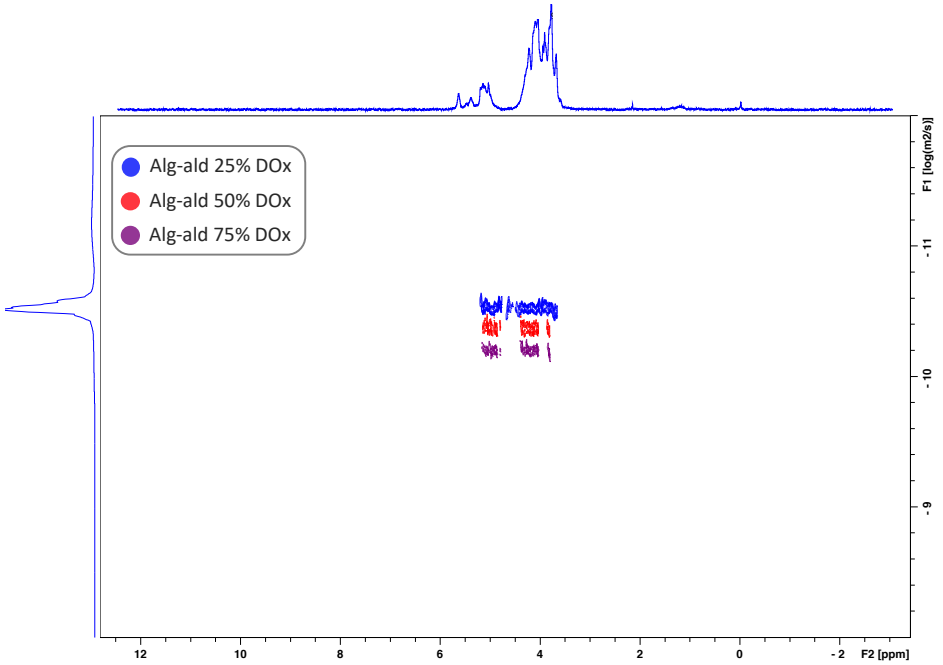

Fig. 11. DOSY Spectra of alginate and alg-ald (25%, 50% and 75% DOx).

The DOSY NMR Spectra (Fig. 11) shows the diffusability of alginates with three different levels of oxidation. As expected, the Alg-ald **2** with less oxidation (25% DOx) showed a slower diffusion, and the Alg-ald with the most oxidation (75% DOx) had a faster diffusion. The diffusion coefficients of the alginate aldehyde at 25% DOx, 50% DOx, and 75% DOx were approximately 1.021 m^2/s, 1.017 m^2/s, 1.009 m^2/s respectively. Oxidation breaks some of the polymeric backbone of the alginate, leading to shorter chains and reduced polymer molecular weight with larger diffusion coefficients.[77,78]

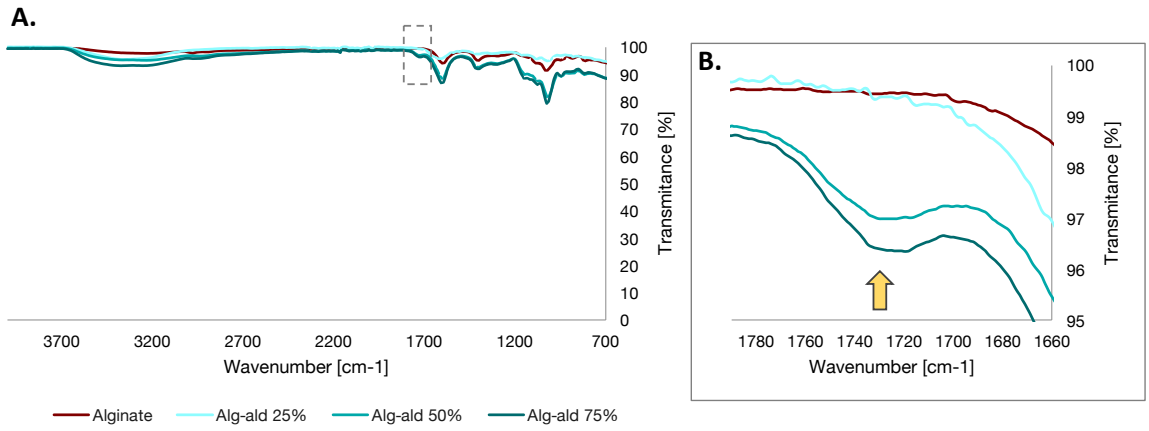

Fig. 12. A. FT-IR Spectra of alginate and alg-ald **2** (25%, 50% and 75% DOx). **B.** Closeup of the FT-IR spectrum range of interest, where the aldehyde peaks appear.

In the FT-IR Spectra (Fig. 12), bands were observed to increase around 1730 cm^{-1} with increasing DOx. An absorbance between 1720 cm^{-1} and 1740 cm^{-1} corresponds to the C=O stretching of aldehydes, further confirming the successful oxidation of the alginate backbone.

2.1.2 Reproducing Alginate Alkoxyamine (alg-AA) 7 developed in the Roh Group[34]

To reproduce the alkoxyamine-alginate previously developed by the Roh group, four steps were necessary (Fig. 13). First, sodium alginate was treated with tetrabutylammonium hydroxide (TBAOH), which exchanged the counter cation for a tetrabutyl ammonium. This was necessary to provide the alginate with slight solubility in organic solvents for the

subsequent steps. Next, a Mitsunobu reaction was performed with triphenylphosphine (PPh_3), Diethyl Azodicarboxylate DEAD, and N-hydroxyphthalimide to convert an alcohol to an alkoxyamine. Then, the phthalimide was deprotected with hydrazine monohydrate, tetrabutylammonium fluoride (TBAF) and tetrahydrofuran (THF). Finally, the product was purified via dialysis against NaCl-saturated water for 2 days to replace TBA^+ with Na^+, and then it was dialyzed against DI H_2O for 3 days to purify the product. This whole process took 14 days and there was no way to monitor the reaction at intermediate points. The final product **7** was characterized using ^1H NMR.

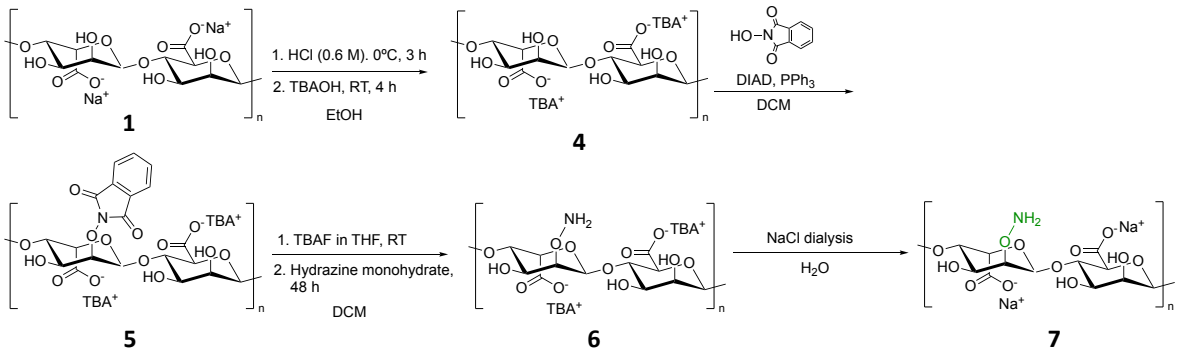

Fig. 13. Synthesis of Sodium Alginate Alkoxyamine.

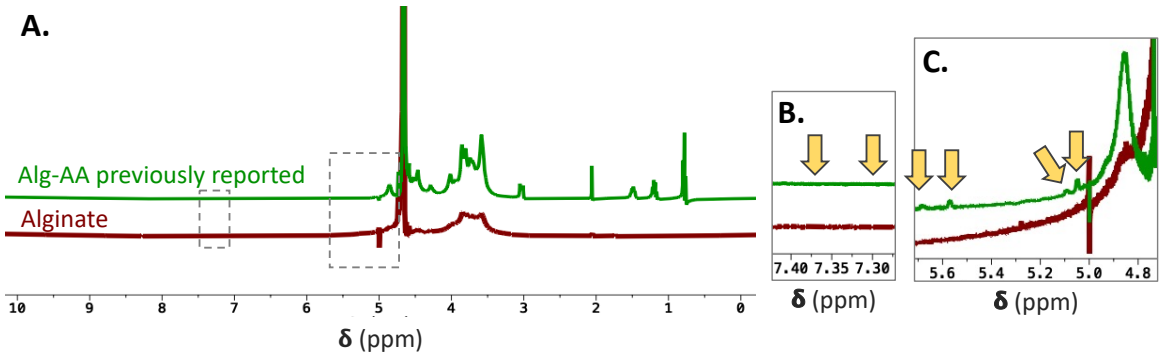

Fig. 14. A. ^1H NMR Spectra of alginate and the reproduced Alg-AA **X**. **B.** Closeup of a chemical shift range of interest, where the alkoxyamine peaks are expected. **C.** Closeup of a chemical shift range of interest, where the new peaks of the Alg-AA are expected.

According to the previously reported protocol,[34] in the ^{1}H NMR Spectra of alginate and the expected alkoxyamine alginate (Fig. 14), two peaks at 7.3 ppm and 7.37 ppm were expected but these were not observed in the spectra (Fig. 14. B.). Additionally, four peaks at 5.2 ppm, 5.3 ppm, 5.8 ppm, 5.9 ppm chemical shifts should be present in the Alg-AA spectra and be absent in the alginate spectra.[34] Though the ^{1}H NMR Spectra of the Alg-AA (Fig. 14. C.) revealed four small peaks at 5.05 ppm, 5.1 ppm, 5.6 ppm, and 5.7 ppm, the relatively small intensities made these results inconclusive.

This four step method required a total period of time of 14 days, and the total cost of the reagents to make 1 g of this Alg-AA **7** was approximately $175 USD.

Moreover, the Mitsunobu reaction needed to be performed under strictly anhydrous and deoxygenated conditions and the product requires a laborious purification due to the difficulty of removing the by-products triphenylphosphine oxide and a hydrazine dicarboxylate.[79-81] This translates into a longer and more complicated process that interferes with the scalability of the procedure as well as its translation to non-specialist labs.

2.1.3 Development of a novel route to access an Alginate Alkoxyamine (alg-AA) 3

Given the major drawbacks of the previously reported route to access an alkoxyamine alginate, we opted to develop a novel route and harness the carboxylic acid functional group in the alginate backbone to introduce an alkoxyamine by amide coupling. We first synthesized a phthalimide protected alkoxyamine, which could be directly coupled to sodium alginate, but found this to be difficult to deprotect (Fig. 16). A second approach was therefore attempted synthesizing a Boc protected alkoxyamine and following the previous coupling and deprotection to obtain a novel alginate alkoxyamine with greatly reduced effort (Fig. 21).

a. Phthalimide-protected alkoxyamine.

The synthesis of the required amine bearing a phthalimide protected alkoxyamine **11** was achieved in three steps (Fig. 15). Each molecule was characterised with ^{1}H NMR and ESI/MS.

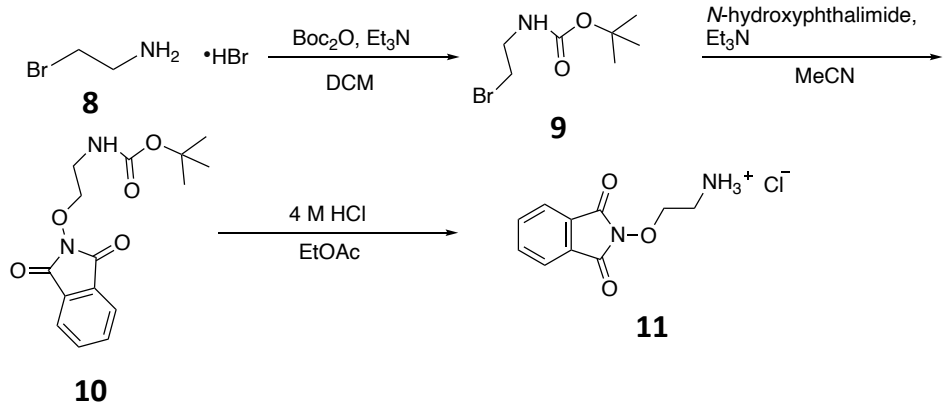

Fig. 15. Synthesis of the phthalimide protected amine.

The initial step was the synthesis of tert-butyl (2-bromoethyl)carbamate **9** employing a procedure previously developed in the group. Triethylamine and Boc_2O were added to a solution of 2-bromoethylamine hydrobromide **1** in DCM at 0 °C, and stirred at RT for 18 hrs. After aqueous work-up, tert-butyl (2-bromoethyl)carbamate **9** product was obtained in an 55% yield.

Then, N-(2-tert-Boc-aminoethoxy)phthalimide **10** was synthesized by mixing **9** with *N*-hydroxyphthalimide in acetonitrile and triethylamine, and stirring at 70 °C for 18 h. After cooling, An aqueous work-up was again sufficient to deliver the product as an off-white solid (50% yield).[82]

The final step was performed by dissolving N-(2--Boc-aminoethoxy)phthalimide **10** in ethyl acetate. Then, a solution of HCl in ethyl acetate was added and stirred at room temperature for 2 h.[83] A white solid of **11** was collected and dried under

reduced pressure by vacuum filtration, and was shown to be the desired product (59% yield).

The cost of the reagents used to make 1 g of the amine **11** was approx. $38 USD, and was synthesized in 4 days without any need for column chromatography.

The prepared amine was coupled to alginate at the carboxylic acid via an amide coupling. NHS and EDC were used as coupling agents based on literature precedent. Three experiments were performed. The first method[84] involved adding EDC to a solution of alginate (1% w/v in DI H_2O), then adding NHS and stirring for 1.5 h. Then, the amine **11** was added at a 1:8 ratio to alginate monomers, and stirred overnight. The coupled alginate was purified by dialysis against DI H_2O. However, this coupling method was not effective, possibly due to hydrolysis of the NHS ester formed as an intermediate, and so a second method[85] (Fig. 16) was attempted. NHS was added to a solution of alginate (1% w/v in PBS), then adding the amine at a 1:8 ratio and stirring for 10 min. This was followed by the addition of EDC and stirring for 25 min. NaOH was then added to cleave any remaining NHS ester and a dialysis against DI H_2O was performed for 4 days, adding NaOH (6 M) and NaCl (4.26 M) twice a day for the first 3 days. Part of the resulting solution was filtered using a 0.45 µm membrane to remove any particulates, and part was not filtered, but there were no observable differences in the NMR of each product. This method was reproduced at 6 different ratios of amine to alginate (2:5, 1:4, 1:8, 1:16, 1:32, 1:96) at a 500 mg scale of alginate.

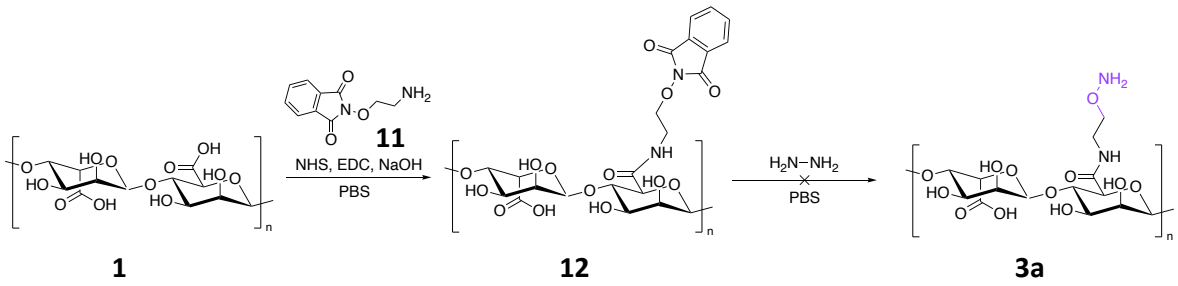

Fig. 16. Scheme of the coupling alginate with the amine protected with the phthalimide group **12**, and the deprotection to form Alg-AA **3a**.

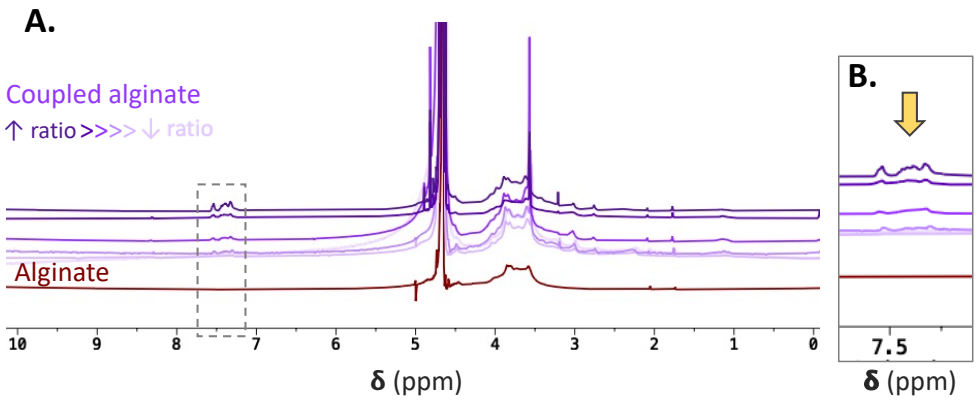

Fig. 17. A. ^{1}H NMR Spectra of alginate and the coupled alginate **12** at six different coupling ratios (darkest tone represents the highest coupling ratio of 2:5, descending to a lightest hue representing the lowest coupling ratio of 1:96) compared to alginate. **B.** Closeup of a chemical shift range of interest, where the *phthal* peaks appear with intensities correlating to the coupling ratio.

The ^{1}H NMR spectra of the six coupled alginate molecules **12** (Fig. 17) showed a new set of peaks around 7.4 ppm corresponding to the phthalimide protecting group, absent in the alginate spectra. Also, the intensity of the peak increased proportionally to the coupling ratio as would be expected with increasing functionalisation.

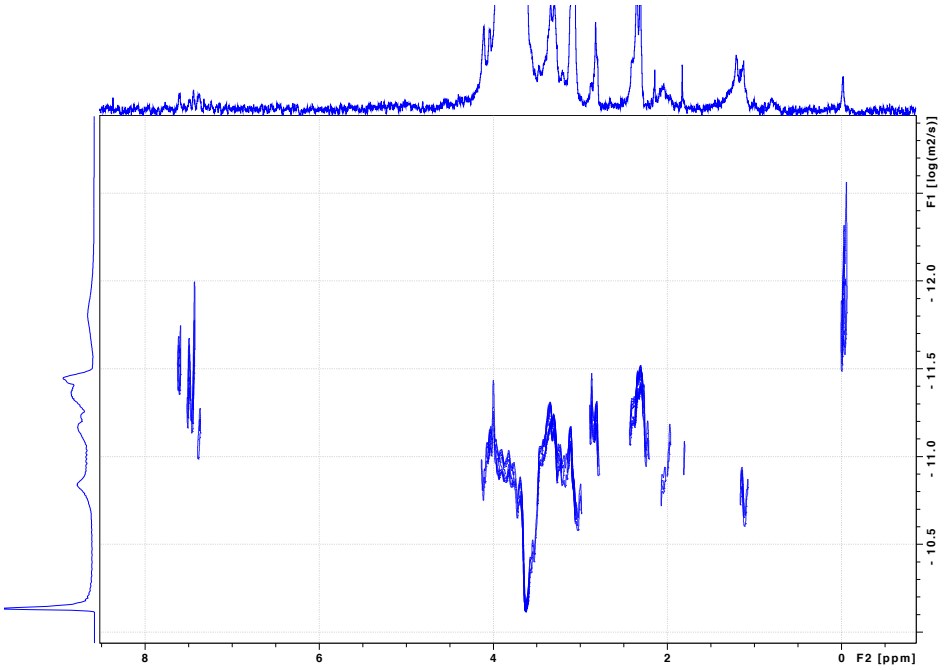

Fig. 18. DOSY NMR Spectra of alginate and alg-AA-phthalimide **12** at 1:96 coupling ratio.

The DOSY NMR Spectra of the coupled alginate (alg-AA-phthalimide) **12** at the lowest coupling ratio (1:96) (Fig. 18) showed that the phthalimide peaks were diffusing at a similar rate to the alginate backbone (diffusion coefficient of around 1.041 m^2/s), which suggests that the amine was successfully coupled. Analogous results were obtained across the six coupling ratios.

To deprotect the phthalimide group hydrazine monohydrate was added and stirred for 72 h, followed by purification by dialysis against tap water for 3 days.

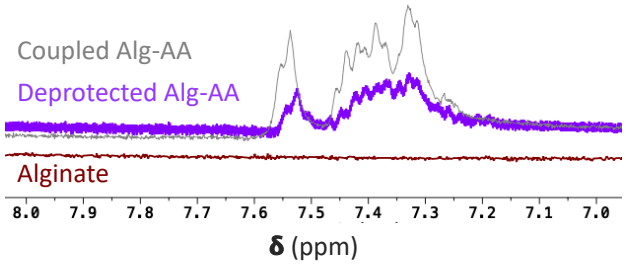

Fig. 19. ^{1}H NMR Spectra of alginate, coupled alginate **12** (2:5 ratio), and deprotected alg-AA **3a**.

The ^{1}H NMR spectra of the coupled alginate molecule **12** compared to the deprotected alg-AA and the alginate (Fig. 19) showed that the deprotection was incomplete. This likely occurred due to the inefficient performance of the hydrazine monohydrate in aqueous conditions.[86] It is not possible to perform hydrazine lysis in organic solvents as traditionally used for *Phthal* deprotection, due to the insolubility of alginate in these solvents.

The synthesis of the new Alg-AA **3a** was made in 11 days, and the total cost of the reagents using the synthesized amine **11** to make 1 g of this new Alg-AA **3a** was approximately $645 USD. This corresponds to a reduction in the costs of the reagents by 7% and the time by 21% in comparison to the previously reported Alg-AA **7**. However, our inability to deprotect the product necessitated the development of an alternative route.

b. Second approach: exploring a Boc-protected alkoxyamine.

Since the deprotection of the phthalimide protecting group was challenging, an amine protected with a Boc group was synthesized, coupled to alginate, and deprotected, to obtain alg-AA.

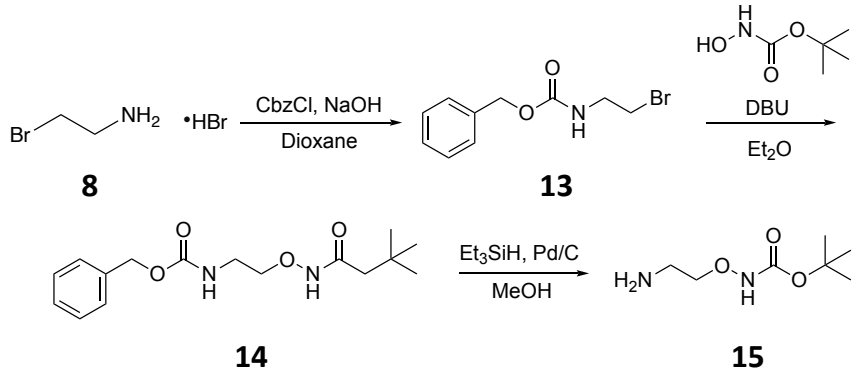

Fig. 20. Synthesis of the Boc protected amine.

To synthesize the amine (Fig. 20), 2-bromoethylamine hydrobromide **8** was dissolved in dioxane at 4 °C, and mixed with sodium hydroxide. Then benzyl chloroformate was added dropwise and stirred at 0 °C for 30 min and then for 18 h at RT. After work-up the product was obtained as a colourless oil of product **13** (the compound was impure).

The product **13** was added to a solution of N-Boc-hydroxylamine in a mixture of Et_2O and DBU, and stirred overnight. After aqueous work up the residue was purified by flash column chromatography giving **14** as a transparent oil with a yield of 11.8%.

To deprotect the Cbz group, **14** was dissolved in MeOH and Chloroform was added. The solution was purged with Argon (Ar) gas and the mixture was treated with Pd/C 5%. Triethylsilane was added dropwise, and the solution was stirred for 1 h. Then, the solution was filtered through Celite and The filtrate was evaporated to dryness to obtain product **15** with inert deprotection side products which were expected not to interfere with the next step.

The amine was produced in 5 days, and the cost of the reagents to produce it was approx. $455 USD per 1 g due to the petroleum ether in the column chromatography, and approximately $130 USD without taking into account the column chromatography. The cost of commercially available options (CAS Number 894414-38-1) for 1 g start at $657 USD.

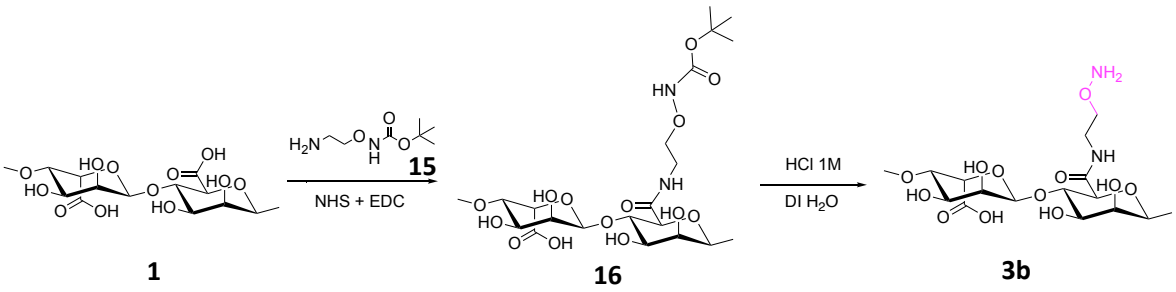

Fig. 21. Scheme of the coupling alginate with the amine protected with the Boc group **15**, and the deprotection to form Alg-AA **3b**.

The Amine **15** was coupled to alginate by following the successful route used for the synthesis of the Phth-protected alkoxyamine alginate (Fig. 21). The resulting solution was purified by dialysis against DI H_2O for 3 days, and the product was lyophilised and stored at -20 °C.

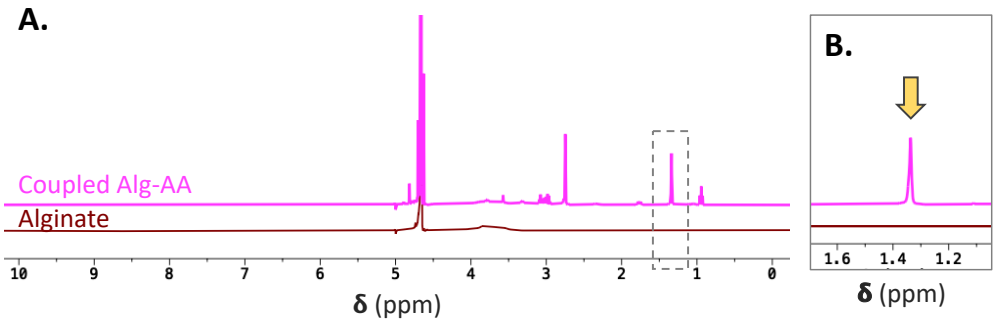

Fig. 22. ^{1}H NMR Spectra of alginate and coupled alginate **16** (2:5 ratio).

A Boc peak at around 1.4 ppm was observed in the ^{1}H NMR Spectrum of the coupled alginate **16** (Fig. 22), confirming the successful coupling of the Boc protected amine to the alginate.

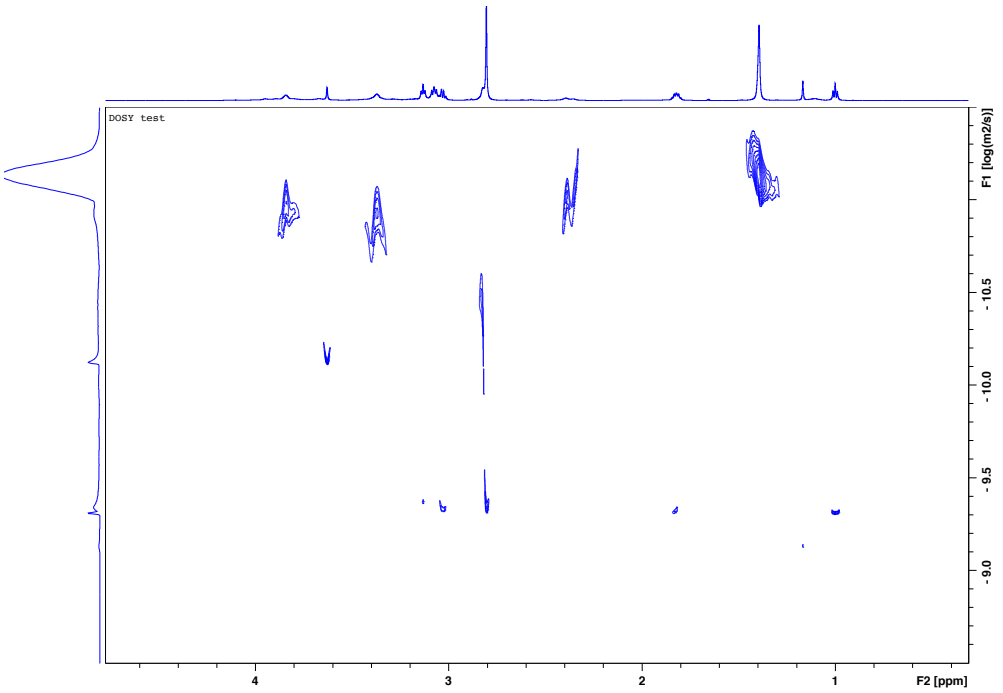

Fig. 23. DOSY NMR Spectra of alginate and coupled Alg-AA **16**.

The DOSY NMR of the alginate coupled to the Boc protected amine **16** (Fig. 23), showed that the peak of the Boc group had the same diffusion coefficient as the alginate of ~1.045 m^2/s, which confirmed the covalent attachment.

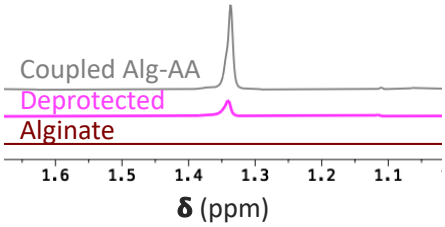

Fig. 24. ^{1}H NMR Spectra of alginate, coupled alginate **16** (2:5 ratio), and deprotected alg-AA **3b** .

The deprotection of the Boc group easily occurred under acidic conditions, in this case we used HCl (1 M). In the ^{1}H NMR spectra of the deprotected alg-AA **3b**, a large reduction was observed in the intensity of the Boc peak at ~1.4 ppm though

a small amount remined (Fig. 24). Despite this, the majority of the alkoxyamine was now accessible for gelation, and this material was moved forward into subsequent parts of the project. This product was not quantified due to noise in the spectrum.

The synthesis of the new Alg-AA **3b** was achieved in a total of 9 days, and the total cost of the reagents to make 1 g of this new Alg-AA **3b** was approximately $190 USD and approximately $78 USD without taking into account the column chromatography of the amine. This resulted in a reduction of the costs of the reagents by up to 55%, and the time by 36% in comparison to the previously reported Alg-AA **7**. Moreover, much of this time was spent synthesising the Boc-protected alkoxyamine, which could be validated at each time point, and for which scale-up is highly feasible, greatly reducing the time and effort required to generate an alkoxyamine functionalised alginate relevant to challenging and poorly reproducible literature procedures.

2.2 Alginate Hydrogels

2.2.1 Ionically Crosslinked Alginate Hydrogels

Alginate hydrogels ionically crosslinked with calcium ions were used as a control to compare with the oxime crosslinked alginate hydrogels. Optimisation of the ionic gelation process was performed to allow accurate comparison to the oxime gels.

Hydrogel formation addition studies

To understand the gelation rate and the shaping of the ionically crosslinked alginate hydrogels, two addition experiments were designed. The first studied four different ratios of alginate to calcium ions, as well as the order of addition. The second experiment considered three different forms of mixing. The hydrogels were prepared by the *in-situ* gelation of alginate with calcium.[87,88]

The first qualitative experiment consisted of 40 hydrogels (Fig. 25) using a constant volume of $CaSO_4$ (dispersed in DI H_2O) and variable amounts of alginate. 20 hydrogels were prepared in a polystyrene 96-well plate (rows A-D, columns 1-5) by adding a $CaSO_4$ stock solution (16% w/v in DI H_2O) on top of an alginate stock solution (1% w/v in DI H_2O), with 5 replicates made from differing ratios (1:1, 3:2, 1:2, 2:1). On the same plate, 10 hydrogels were prepared by reversing the addition, adding $CaSO_4$ to the alginate (rows A, B). A further10 hydrogels were prepared with different addition methods: the second component was added on top (columns 8, 9), pipetted inside the other (column 10), or mixed into the other (columns 11, 12).

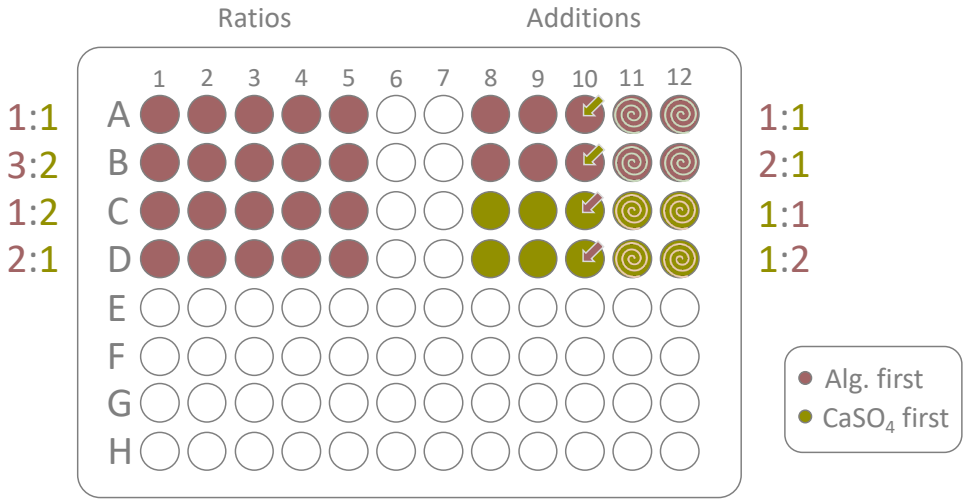

Fig. 25. Organization of the plates. In the maroon coloured wells, alginate was added first and $CaSO_4$ was added next. In the dark wood-green coloured wells, the order of addition was the opposite. Hydrogels in columns 1-5 had a variation of ratios, and in the columns 8-12 the addition methods were varied. The arrow in column 10 represents the addition inside of the solution, and the spirals on columns 11-12 represent mixing motions.

The hydrogels formed at different alginate to $CaSO_4$ ratios showed that the size of the hydrogels was correlated to the amount of alginate present, independent of the amount of $CaSO_4$ within the range tested (Fig. 26). Theoretically, alginate can absorb 17 to 40 times its weight in water. Within a 200 µL gel there was 0.5 mg of alginate, so an absorption of 0.68

mL and up to 4 mL of DI H_2O would have been expected. Since the volume of the gels was only 200 µL, all of the gelation volume would have been theoretically retained.

When $CaSO_4$ was added to an alginate stock, cylindrical hydrogels with weak or uncrosslinked interiors were formed (Fig. 26 B. rows A, B). When addition was reversed and alginate was added to the calcium stock (Fig. 26 B. rows C, D), stronger but smaller gels were formed with uncontrolled shapes depending on the addition method. When alginate was released on top of the calcium solution (Fig. 26 B. rows C, D and columns 8, 9), a "droplike" shape was formed,[89] as the alginate gelled rapidly as it came in contact with the calcium ions on the surface. The technique of pipetting the solution into the other (Fig. 26 B. column 10), formed small compact hydrogels with uniform consistency but heterogeneous surface. The hydrogels formed with mixing similarly formed very heterogeneous structures.

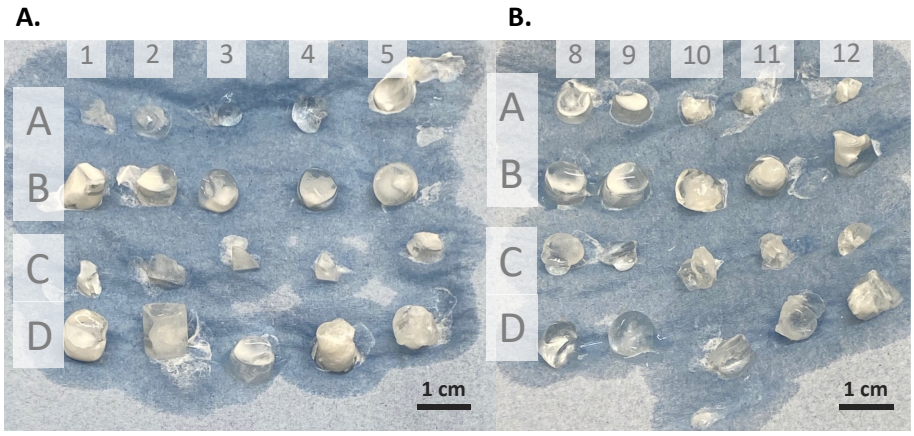

Fig. 26. Ionically crosslinked alginate hydrogels. **A.** Hydrogels crosslinked at four different alginate to $CaSO_4$ ratios. Row A at 1:1, row B at 3:2, row C at 2:1 with the smallest hydrogels, and row D at 1:2 with the biggest hydrogels. **B.** Hydrogels with different addition methods. In rows A, B, the $CaSO_4$ solution was added on top of the alginate solution, whereas in rows C, D, the $CaSO_4$ solution was added first. In columns 8,9 the second solution was added on top, in 10, it was pipetted into the first solution, and in columns 11, 12, it was mixed.

Next, in a polystyrene 96-well plate, 3 hydrogels were made using $CaCl_2$ stock solution, rather than $CaSO_4$, in DI H_2O (5% w/v) as a crosslinker. The hydrogels were prepared in a 1:1 alginate to crosslinker ratio. $CaCl_2$ solution was pipetted on top of the alginate solution. For the first hydrogel, the calcium solution was added dropwise on top, while the second hydrogel was prepared by adding the crosslinking solution to the side of the well with a slow and constant flow. Finally, for the third hydrogel the $CaCl_2$ solution was added in a single fast motion on top.

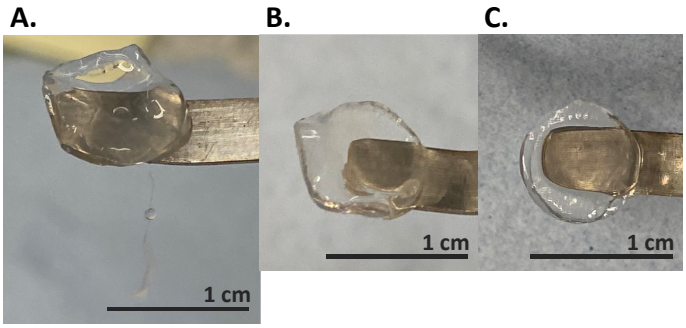

Fig. 27. Ionically crosslinked alginate hydrogels. **A.** Hydrogel resulting from $CaCl_2$ added dropwise on top of alginate. **B.** Hydrogel resulting from $CaCl_2$ added to the side of the well with a slow and constant flow. **C.** Hydrogel resulting from $CaCl_2$ quickly added on top of alginate.

Two of the hydrogels (Fig. 27 A., B.) had a very uneven and disrupted form. The hydrogel formed via dropwise $CaCl_2$ addition (Fig. 27 A.) had a string of hydrogel attached to the side. The fast addition of crosslinker solution (Fig. 27 C.) unexpectedly resulted in a hydrogel with a uniform cylindrical shape.

When using both calcium sources the ionically crosslinked hydrogels formed heterogeneous shapes due to the high gelation rates. Additionally, after a short period of time (less than 24 h), the gels collapsed. The $CaCl_2$ solution formed alginate hydrogels with more controllable shapes than when $CaSO_4$ was used, but the alginate crosslinked with $CaSO_4$ was mechanically stronger on the exterior. Due to the heterogeneity of dispersed $CaSO_4$ in DI H_2O, it was harder to control the distribution of the calcium ions. For this reason, using $CaCl_2$

solution in DI H_2O was easier to control and resulted in hydrogels with more homogeneous shapes. Additionally, after a short period of time (less than 24 h), the gels collapsed because of the ion leaching that broke the ionic crosslinking.

Moulds and materials to shape the hydrogels

Cylindrical moulds of different materials and bases, of equal dimensions (8 mm diameter and an arbitrary variable height between 3-20 mm), were designed to produce reproducible ionically crosslinked gels. Attempting to make gels within a 96-well plate led to a drop-like geometries. The hydrogels with the calcium solution added on top of the alginate (Fig. 28 A.) were expected to result in a cylindrical geometry, which was not observed. It was thought the speed and/or force of the addition of the calcium solution could have affected the gelation of the alginate into a spherical base.

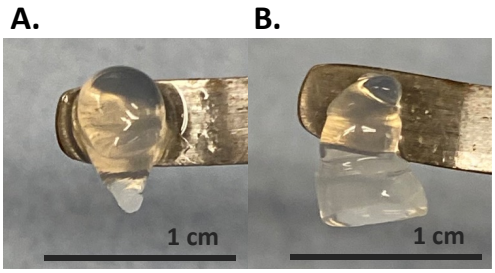

Fig. 28. Ionically crosslinked alginate hydrogels. **A.** $CaCl_2$ solution added on top of alginate. **B.** Alginate added after the calcium solution.

All the resulting hydrogels (Fig. 28) obtained However, depending on specific conditions and varying factors, alginate beads can acquire tear or pear shapes when dropped into the calcium solution,[89] which was observed on the gels with the opposite order of addition (Fig. 28 A.). Moreover, this plate limited our ability to obtain the gels free of the plate due to the rigidity of the plate.

In order to address this, the polystyrene 96-well plate was modified by removing the lower base and used to form gels on a detachable aluminium base, a polystyrene base, or a silicon

base. An additional 96-well plate was designed made of Polytetrafluoroethylene (PTFE), a material with high hydrophobicity and low friction coefficient, which we hypothesised would minimize hydrogel adhesion. However, despite the application of a weight to try and seal the plate-base interface, all these moulds resulted in leaking (Fig. 29 A,B) that affected gelation. Due to this leaking, many hydrogels fused together and acquired asymmetrical shapes (Fig. 29 C,D).

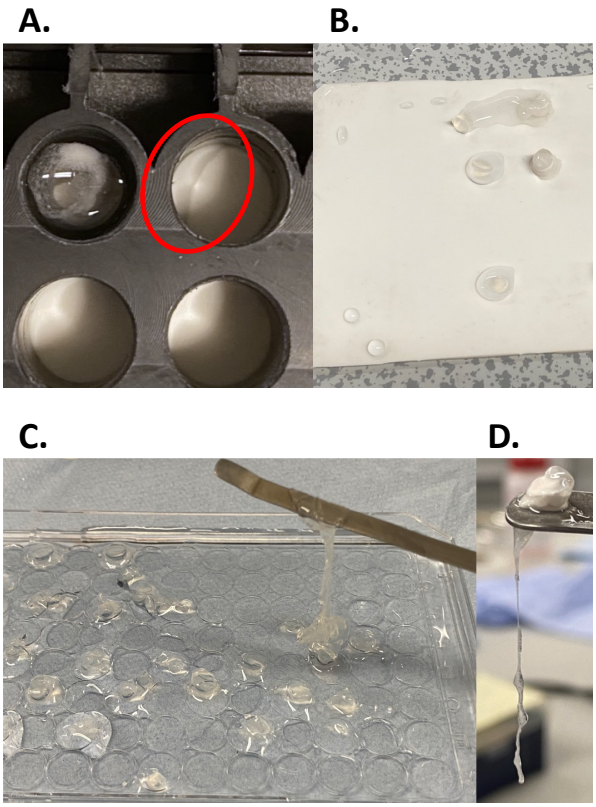

Fig. 29. Gelation problems in hollow moulds. **A, B.** Leaking. **C,D.** Fused hydrogels.

Finally, silicone moulds were successfully custom made by the group to achieve the intended proportions and eliminate the rigidity and leakages. The moulds (Fig. 30) were made following the instructions of a silicone mold making kit, and a bioplastic was used as a negative. A hydrogel was prepared in the mould by adding alginate into $CaCl_2$ solution, round sphere gel formed suspended in aqueous solution.

Fig. 30. Custom silicone moulds. **A.** Silicone mold making kit. **B.** Three step process: adding the silicone mixture (1A:1B mix ratio part A and Part B), using the negative to form the cylinder interior, the final mould.

2.2.2 Novel Oxime Crosslinked Alginate Hydrogels

Ionically crosslinking of components: alg-ald 2 and alg-AA 3b

Before preparing the new oxime crosslinked hydrogels, the behaviour of the two independent components, alginate aldehyde **2** and alginate alkoxyamine **3b**, were studied. First, their ionic crosslinking was studied. Alg-ald at three DOx (25%, 50%, 75%) was easily dissolved in DI H_2O at a 1% w/v concentration. The pH of the alg-ald **2** 50% DOx solution was 4.4. Alg-AA **3b** was also dissolved with vigorous mixing in DI H_2O at a 1% w/v to give a solution with pH 2.7. These four solutions were independently mixed with $CaSO_4$ or $CaCl_2$ stock solutions. The solutions did not gel at time 0, indicating gelation was slowed relative to sodium alginate. This may confirm a change in the alginate structure, or may have been due to pH effects. After 6 h and 30 h the solutions were still in a liquid state, qualitatively meaning all the analysed molecules did not ionically crosslink with calcium ions.

Oxime Crosslinked hydrogels In DI H_2O

Alg-ald **2** at a 50% DOx and alg-AA **3b** 1% w/v solutions were made in DI H_2O. in a polystyrene 96-well plate, alg-ad solution was added on top of alg-AA solution at three ratios (1:2, 1:1, 2:1) and in replicates. Under these conditions, no gelation was observed after 0, 4 or 24 hrs.

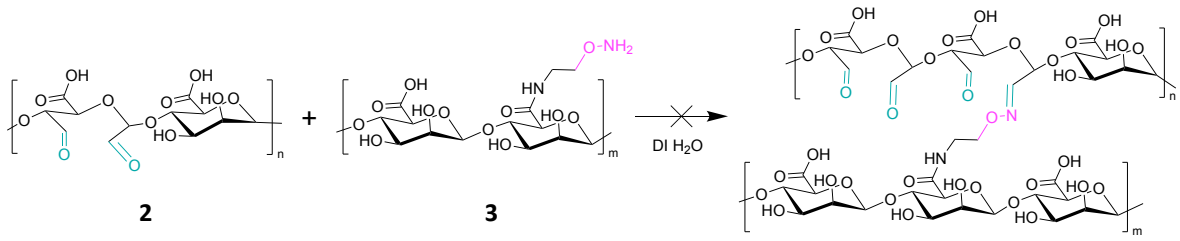

Fig. 31. Scheme of the oxime crosslinked alginate hydrogels via alg-ald and novel alg-AA in DI H_2O.

Comparing the previously reported hydrogels and the oxime hydrogels prepared with the alg-AA 3b synthesized with the new route

We hypothesized that the pH of the reaction mixture might be preventing gel formation. We therefore attempted gelation at a range of different pHs. As a control, the gels were compared to ionically crosslinked gels of sodium alginate (Fig. 32).

Gelation was attempted by dissolving alg-ald **2** (only 50% DOx) and alg-AA **3b** in a 1% w/v concentration in three different buffers: PBS, or pH 6 or pH 8 phosphate buffers. Observations of the 8 hydrogels were made for 13 days.

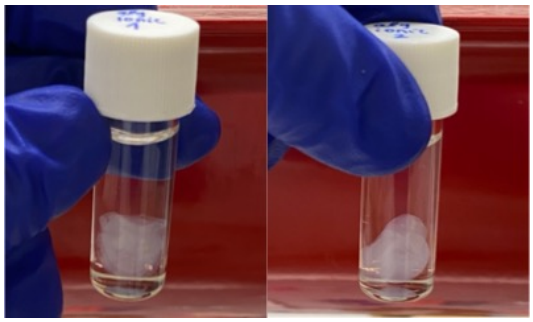

Fig. 32. Two ionically crosslinked alginate hydrogels in DI H_2O.

After adding the calcium solution, the ionically crosslinked gels quickly formed in heterogeneous shapes suspended in an aqueous phase (Fig. 32). After 1 day, these were noticeably collapsing and losing their form. Both gels reduced their size and formed a clump of solid alginate in aqueous solution.

In contrast, our attempts to form gels following the previously reported methods of Roh, made with 1% w/v solutions of alginate, did not gel after 15 min or during a period of 14 days, except in PBS where a very mechanically weak gel formed slowly (Fig. 33, B). On the contrary, using our novel hydroxylamine alginate, spontaneous gelation took place in under 15 min, and after 13 days the materials remained gelled. As judged by a vial inversion test, gels were formed more robustly at pH 6 than pH 8, which was expected because the oxime formation is favourable in acidic conditions (Fig. 33, A).[34]

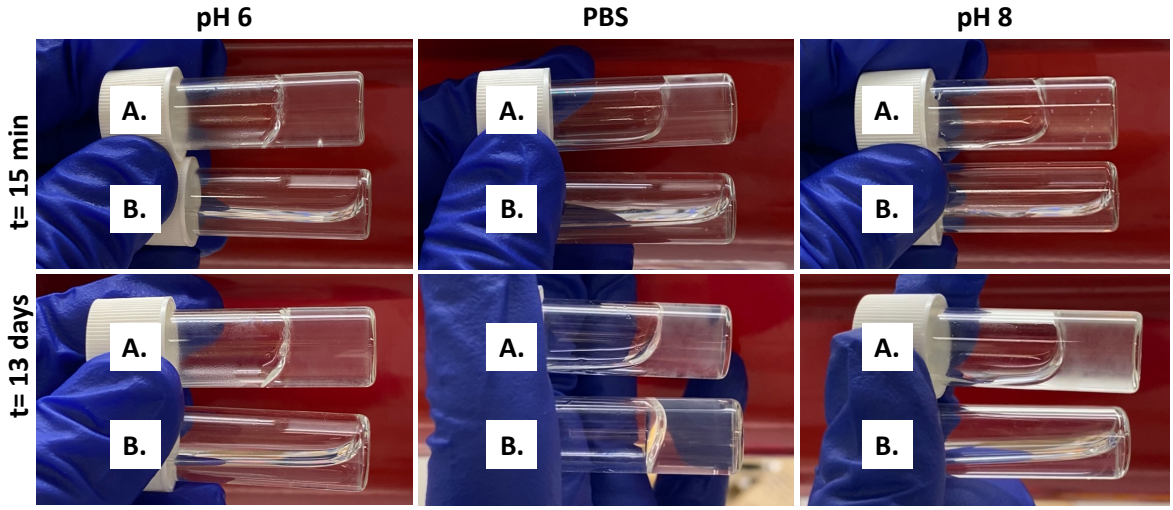

Fig. 33. Oxime crosslinked alginate hydrogels via new alg-AA route and previously reported. First row (after 15 min): all the novel developed hydrogels (**A.**) were formed and the previously reported (**B.**) were in liquid solution. Second row (after 13 days): the novel developed hydrogels were still gelled, and only the previously reported formed in PBS gelled and the other were still liquid.

In general, oxime crosslinked hydrogels could be formed with more control when compared to the ionically crosslinked ones, because in the first hydrogels all the amount of the two

solutions (alg-ald and alg-AA) formed a gel with the shape of the mould, whereas in the second hydrogels only the Calcium ions dissolved in the solvent formed ionic crosslinks in the alginate solution, leaving an aqueous phase surrounding the not-moulded gels. Moreover, through our novel design we were able to form gels at low concentrations of 1% w/v in a period of 15 min, while the reproduced hydrogels from the Roh group did not gel at 1% w/v in this time.[34] It is important to note that the hydrogels reported[34] were prepared at higher concentrations (2% to 5% v/v) and gelled under these conditions, which represents an advantage of the capability of the novel hydrogels to gel at a lower concentration.

Rheological studies of novel oxime crosslinked hydrogels

We next went on to study rheological properties of the oxime hydrogels we had formed. Hydrogels were prepared at a 1:1 ratio of alg-ald 50% DOx **2** to alg-AA **3b** solutions at a 1% w/v in in PBS or pH 6 or 8 phosphate buffer (Fig. 34). After ~20 h, oscillatory shear rheological experiments were performed to measure the mechanical properties of the hydrogels. First, an amplitude sweep was performed to determine and the linear viscoelastic region, followed by a frequency sweep. The measurements were made in triplicate and the average values were reported.

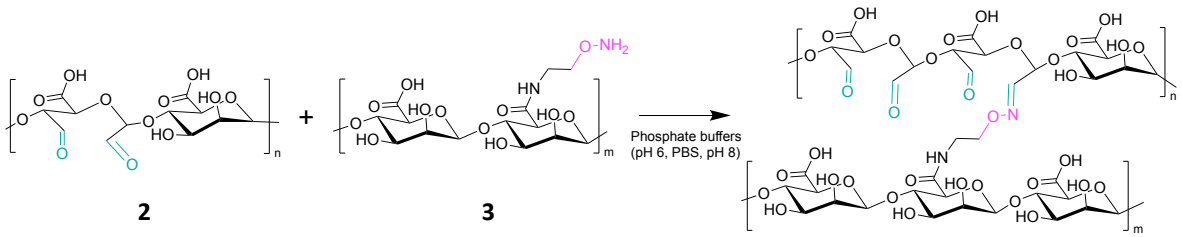

2 **3**

Fig. 34. Scheme of the oxime crosslinked alginate hydrogels via alg-ald and novel alg-AA in three different phosphate buffers: pH 6, PBS, pH 8.

Table 1. Physical properties of the gels determined using oscillatory rheometry with a parallel plate geometry, for the oxime crosslinked hydrogels. The G'/G" crossover points correspond to the % shear strain at which G'=G''.

Gel	G' (Pa)	G'' (Pa)	G'/G'' crossover
pH 6	226.8 ± 17.4	29.2 ± 4.9	~8%
PBS	87.4 ± 7.5	6.1 ± 3.0	~21%
pH 8	176.8 ± 6.7	15.7 ± 4.2	~21%

All hydrogels prepared at three different pH conditions gelled (G'>G''). The G' value of the hydrogels prepared in acidic conditions (pH 6) had a value of 226.8 ± 17.4 Pa, the ones in neutral conditions (in PBS) had the lowest G' value at 87.4 ± 7.5 Pa, and the hydrogels at basic pH (pH 8) had a G' value of 176.8 ± 6.7 Pa. As expected, this means the hydrogel prepared under acidic buffer favoured the formation of oxime crosslinking and formed stiffer gels.[34] Soft tissue elasticity ranges from 0.1 to 15 kPa approximately,[41,90] and the hydrogels prepared in pH 6 and pH 8 buffers are in this range.

2.3 Economic Analysis and Commentary

To address our goal of designing an affordable hydrogel and report the costs of the project, a basic economic analysis was made by calculating the price of the amount of solvents and reagents used in each experiment. The price used was the commercial value in Great Britain Pounds (£, GBP) from 2022 found on the website of each supplier, and converted to USD using representative exchange rates from May-June 2022, approximately £1 ≈ $1.27 USD. A total value of the cost of reagents was estimated to have a clear idea of one of the costs of this project. The approximate total value was ~ £450 or ~ $570 USD.

An accurate, but also low-cost platform that *replaces* animal testing, contributes to biomedical research progress and diversification by transforming into an inclusive branch of science. Additionally, reporting the costs of research projects creates awareness of inequalities and needs in the scientific community. To make a comparison and to have an

idea, in 2017/18, the gross medical research expenditure from the Medical Research Council (MRC) at the UK Research and Innovation (UKRI) was £814.1 million (~$912 million USD), but in Colombia, an example of an emerging country, was approximately $10 million USD in 2019 according to Minciencias and Minsalud. Moreover, in an interview with Dr Catalina Pineda, Head of the Biomedical Engineering Program at Universidad CES in Colombia, she states among the limitations of tissue engineering research in emerging countries the marginal restrictions and costs of importing international supplies, like high taxes and currency exchange rates. This ignored inequality represents ~90 times more investment in developed economies but also more access and facilities, therefore a need of developing a scalable, high-calibre and cost-effective models for competitive biomedical research in emerging countries.

3. Conclusions and Future Work

In this project we devised a new route to form oxime crosslinked alginate hydrogels. First, alginate derivatives were synthesized by successfully reproducing a previously reported alginate-alkoxyamine **2** with three degrees of oxidation, and then exploring routes to synthesize an alginate-alkoxyamine **3** by amide coupling at the carboxylic acid. The first approach using an phthalimide **3a** was inefficient due to the aqueous conditions. The following approach, using a Boc protecting group, resulted in the successful synthesis of the alginate-alkoxyamine **3b**.

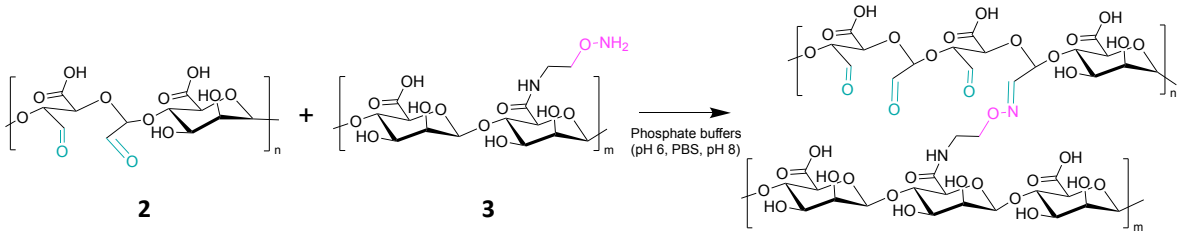

Fig. 34. Scheme of the oxime crosslinked alginate hydrogels via alg-ald and novel alg-AA in three different phosphate buffers: pH 6, PBS, pH 8.

Novel oxime crosslinked alginate hydrogels were prepared by dissolving alg-ald **2** and alg-AA **3b** in DI H_2O first and phosphate buffers next. The hydrogels did not form in aqueous conditions, but the solution gelled at pH 6, pH 7.5, and pH 8, and were still gelled after 13 days (Fig. 33,A). These hydrogels were compared to standard ionically crosslinked alginate hydrogels, which form in high gelation rates and result in gels with irregular shapes. Due to leaching out of the divalent cations, these hydrogels collapse after a period of time. The developed oxime crosslinked hydrogels solved these two well-known issues that ionically crosslinked hydrogels tend to have. Moreover, we compared these novel developed hydrogels with previously reported oxime crosslinked gels (Fig. 33,B). Not only the synthesis of the alginate alkoxyamine **3** was faster and more straightforward than the previously reported alg-AA **7**, but the novel hydrogels at 1% w/v and in phosphate buffers formed in less than 15 min and resisted for the 13 days of the experiment; meanwhile, the previously

reported prepared at the same conditions did not gel after 15 min, and only the one at neutral pH formed after days.

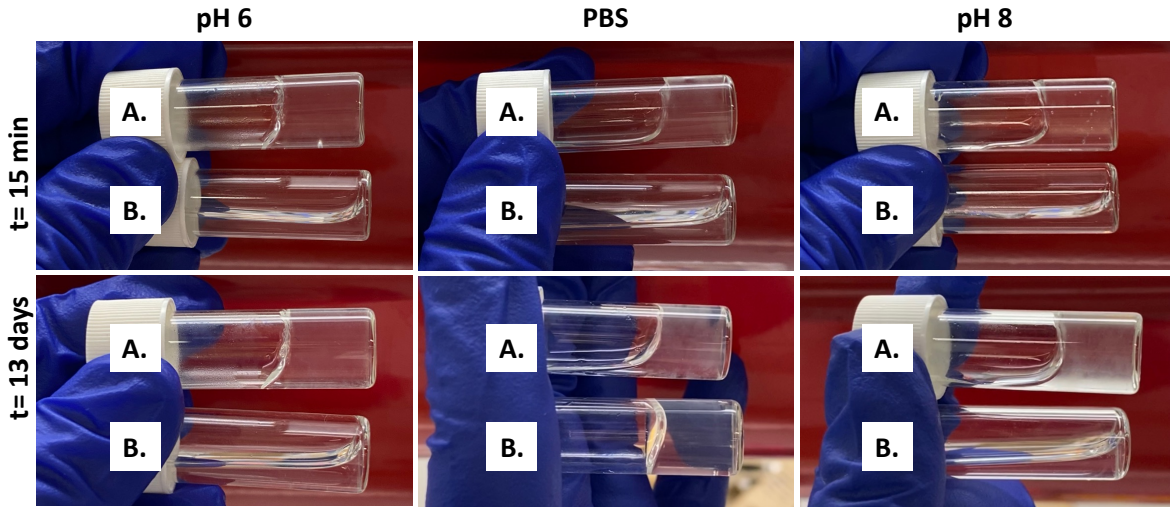

Fig. 33. Oxime crosslinked alginate hydrogels via new alg-AA route and previously reported. First row (after 15 min): all the novel developed hydrogels (**A.**) were formed and the previously reported (**B.**) were in liquid solution. Second row (after 13 days): the novel developed hydrogels were still gelled, and only the previously reported formed in PBS gelled and the other were still liquid.

By implementing our strategy we also achieved our initial goals of developing a low cost and sustainable material that can be engineered further to mimic human soft tissues. The rheological studies confirmed that the hydrogels prepared at 1% w/v (1:1 ratio) in pH 6 and pH8 buffers have elastic modulus within the range of native soft tissues. Future work towards mimicking the key characteristics of the ECM in soft tissues must be oriented towards studies like functionalising it with bioactive ligands and cell-adhesive peptides, variations of the measurements used, cell culture experiments, and studying the effect of temperature and aniline as a catalysts. Our developed dynamic material represents a step towards creating a smarter platform that serves as an accurate alternative to animal models.

Furthermore, we confirmed that it is possible to develop a high quality, dynamic and low cost biomaterial that transforms research into a more inclusive and welcoming environment to groups from multiple economic backgrounds and limited financial resources. It is very important to create awareness of this need, but also to become more inclusive in the biomedical research community. Also, it is important to explore ways to report costs and request this when publishing biomedical research projects.

4. Experimental

4.1 General Considerations

4.1.1 Synthesis of Alginate Derivatives

All solvents and reagents were acquired from standard commercial suppliers and used as received without prior purification. Alginic acid sodium salt from brown algae (Sodium Alginate NaAlg, 21,900 molecular size, estimated molecular weight: 250,000 - 350,000), of medium viscosity (≥2,000 cP, 2 %(25 °C)(lit.)) was purchased from Sigma-Aldrich (CAS Number 90005-38-3, A2033, Lot # SLCF1478), and has a mannuronic acid to guluronic acid ratio of approximately 1.56 (60-70% M-block and 30-40% G-block). Lyophilized products were stored at -18°C. All aqueous solutions were prepared using deionised water (DI H_2O). Brine refers to a saturated solution of sodium chloride (NaCl).

Dialysis purification was performed with DI H_2O, unless stated otherwise. The membranes used were Thermo Fisher SnakeSkin™ Dialysis Tubing, 10K MWCO, with 16 mm or 35 mm tube diameter. Water changing varied in multiple intervals of around 2 h to overnight. Purification of the same molecules at different concentrations or degrees of modification were dialyzed in the same water container. Thin Layer chromatography (TLC) was carried out using aluminium backed sheets coated with 60 F_{254} silica gel (Merck). Visualization of the silica plates was made using a UV lamp (λmax = 254, 302, or 366 nm).

Proton nuclear magnetic resonance (^{1}H NMR) spectra were recorded on a Jeol ECX-400 (400 MHz). Due to the large size of the polymeric molecule of alginate and modified alginate, 1024 scans were collected to increase the signal-to-noise ratio, unless indicated otherwise. Mestrelab Mnova 14.0.0 NMR software was used for the analysis of the NMR spectra and the integrals were relative to the smallest peak. DOSY NMR measurements were performed on a 700 mHz Spectrometer, using pulse programs ledbpgppr2s and dstebpgppr3s with water suppression. Infrared (IR) spectra were recorded on a Perkin Elmer UATR Two FT-IR spectrometer. UV-Vis spectra were recorded on a Perkin Elmer Lambda 25 spectrophotometer in a quarts cuvette with a pathlength of 1cm. High resolution

electrospray ionisation (ESI) mass spectra (HRMS) were recorded on a Bruker Campact TOF-MS or a Jeol AccuTOF GCx-plus spectrometer. Flash column chromatography was carried out using Fluka Chemie GmbH silica (220- 440 mesh).

4.1.2 Alginate Hydrogels

Ionically crosslinked alginate hydrogels were made following previously reported protocols.[87,88] Sodium alginate (1% w/v), calcium sulfate (16.5% w/v) and calcium chloride (5% w/v) were dissolved in DI H_2O and stored at room temperature. The alginate and calcium solutions were mixed in various moulds at different ratios and left for different periods of time to gel and form ionically crosslinked hydrogels.

Modified alginate polymers were dissolved initially in DI H_2O or different buffers at 1% w/v and/or 5% w/v, gelled at a 1:1 ratio at different times in glass vials or silicone moulds.

Gel samples for rheology were prepared using silicone moulds previously made to obtain the intended gel dimensions. The silicone moulds were made following the Startso World Mold Making Kit and instructions (20A RTV-2 liquid Silicone Rubber), and Thermoworx Whitemorph bioplastic negative shapes of specific cylindric volume measurements to fit the rheometer geometry. Rheology was measured using oscillatory rheometry in triplicates on a Malvern Instruments Kinexus Pro+ Rheometer fitted with a 8 mm parallel plate geometry at 25°C. During the loading, the experimental gap size (2-8 mm) was set according to the height of each gel, ensuring a complete contact of the gel and the geometry. Amplitude sweep experiments were performed in the range of 0.1-100% strain at 1 Hz frequency to identify the linear viscoelastic region. Frequency sweep experiments were performed between 0.1 and 100 Hz using a shear strain of 0.1%. Photos were taken using an Apple iPhone 11 Pro Wide (ƒ/1.8 aperture) and Telephoto (ƒ/2.0 aperture) cameras. Scaling in the pictures was made with a standard centimetre (cm) ruler.

4.1.3 Economic Analysis and Commentary

A basic economic analysis was made by calculating the price of the amount of solvents and reagents used in each experiment, taking into account the commercial value in Great Britain Pounds (£, GBP) of each package of reagent (value of 2022 found on the website of each supplier, without taking into account any academic institution or alliance discounts). The costs were then converted to USD using representative exchange rates from May to June 2022 (approximately £1 ≈ $1.27 USD). The cost of each molecule synthesized was adjusted to 1 g by linear extrapolation to standardize all the values at this amount. A total value of the cost of reagents was estimated to have a clear idea of one of the costs of this project. For context and to make a comparison, official governmental sources were consulted: The Medical Research Council (MRC) at the UK Research and Innovation (UKRI); Minciencias and Minsalud in Colombia. Dr Catalina Pineda, Head of the Biomedical Engineering Program at Universidad CES (Medellín, Colombia) was also consulted.

4.2 Synthesis of Alginate Derivatives

4.2.1 Alginate Aldehyde (alg-ald) 2

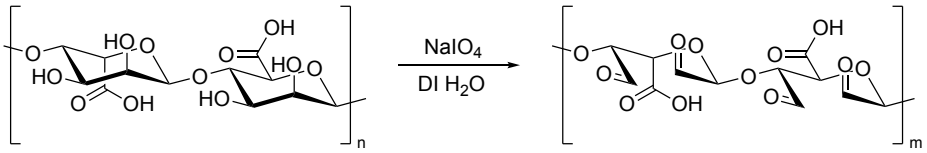

1 **2**

Alginate-Aldehyde (Alg-Ald) **2** with a 25%, 50%, or 75% degrees of oxidation (DOx) was obtained using a previously reported procedure.[34] For the Alg-Ald at 50% DOx, Sodium Alginate **1** (2.00 g) was added to DI H_2O (150 mL) to give a final concentration of 1.3% w/v. Next, sodium metaperiodate (2.09 g, 9.25 mmol) was added. The light-yellow viscous solution was stirred for 18 hr, then purified by dialysis (10k MWCO membrane) against DI H_2O and lyophilized. A yield of 1.1 g (~55%) of 50% DOx alginate was obtained.

For polymers with 25% or 75% Dox an analogous procedure was followed, varying the amount of sodium metaperiodate used. Yields of 1.0 g 25% DOx (~50%) and 1.2 g 75% DOx (~60%) were obtained. The products were isolated as white sponges that were stored at -20 °C until further use.

The Alg-ald **2** was characterized using ^{1}H NMR (integrals are relative to the smallest peak), DOSY NMR, FT-IR. Alg-ald with 0% DOx ^{1}H NMR (400 MHz, D_2O): 3.20-4.30 (m); Alg-ald at 75% DOx ^{1}H NMR (400 MHz, D_2O): 5.43-5.60 (1H, m), 5.25-5.39 (2H, m), 4.78-5.17 (17H, m), 3.93-4.41 (8H, m), 3.69-3.93 (1.5H, m).

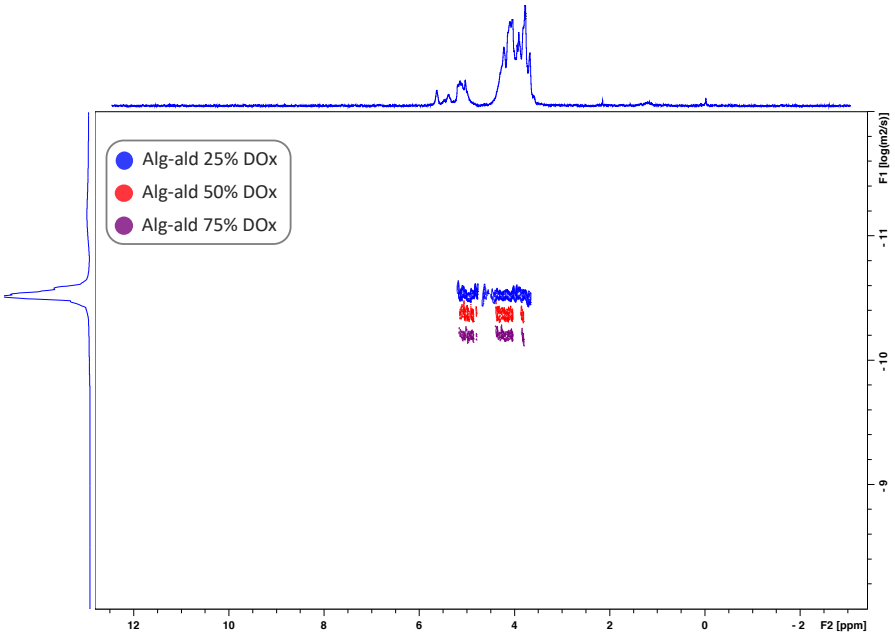

Fig. 35. DOSY Spectra of alginate and alg-ald (25%, 50% and 75% DOx) **2**.

The DOSY NMR (Fig. 35) on the alg-ald 50% DOx **2**, was performed using the pulse program dstebpgppr3s, which uses water suppression, with the parameters: sw 16.2 ppm x 10.2 ppm, TD 32k x 16, diffusion time **Δ** D20 = 0.25s, diffusion gradient length **δ** p30 = 1.5ms.

Lab book references: **AMRR007**, **AMRR014**

4.2.2 Reproducing Alginate Alkoxyamine (alg-AA) 7 developed in the Roh Group[34]

Synthesis of TBA-Alginate (TBA-Alg) 4

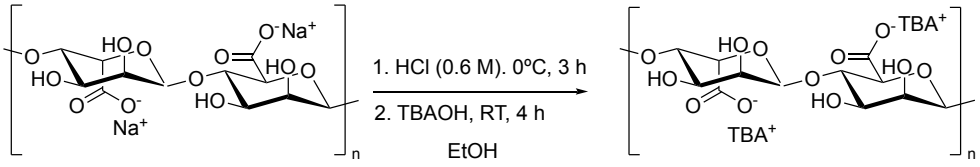

1 **4**

Sodium alginate **1** (8 g) was slowly added to a 1:1 mixture (v/v) of HCl (0.6 M) and ethanol (500 mL), and mixed at 4 °C for 3 h. A cloudy yellow suspension developed. The product was collected by filtration under vacuum, and dried in vacuum at 60 °C overnight. The intermediate alginic acid (6 g, ~75% yield) was dissolved in DI H_2O (170 mL) with vigorous stirring. Tetrabutylammonium hydroxide (TBAOH 40% (w/v in water) was added portionwise until the alginate was solubilized. Dialysis against DI H_2O was performed using a 10k MWCO cellulose membrane for four days. The supernatant was then lyophilised and stored at -20 °C. A total of 4.82 g of TBA-Alg **4** was obtained with a ~60% yield.

Lab book reference: **AMRR004**

Synthesis of TBA-Alginate-Phthalimide (TBA-Alg-*phthal*) 5

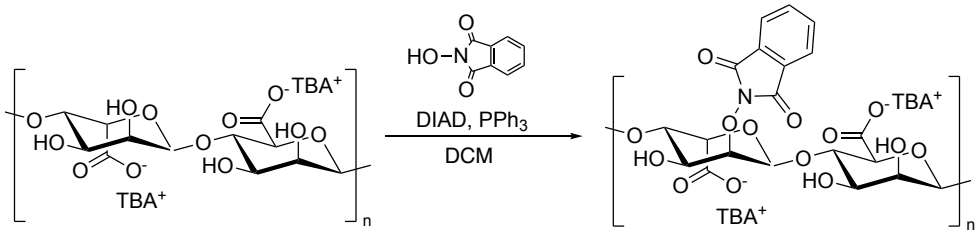

4 **5**

TBA-Alg **4** (0.72 g) was dispersed in DCM (CH_2Cl_2, 165 mL). Triphenylphosphine (4.9 g, 18.68 mmol) was then added, followed by an addition of N-hydroxyphthalimide (3.1 g, 19.00 mmol), resulting in gas formation and a strong yellow colour. The solution was cooled to 4 °C and purged with N_2 gas for 30 min. Next, diisopropyl azodicarboxylate (DIAD, 3.1 mL) was

added dropwise leading to a dark orange colour. The mixture was left stirring for 2 days then filtered under vacuum. The solid was washed with ethanol (~500 mL) and dried under vacuum at 60 °C. A total of 0.59 g of TBA-Alg-*phthal* **5** was obtained, with an ~82% of yield.

Lab book reference: **AMRR009**

Synthesis of TBA-Alginate-Alkoxyamine (TBA-Alg-AA) 6

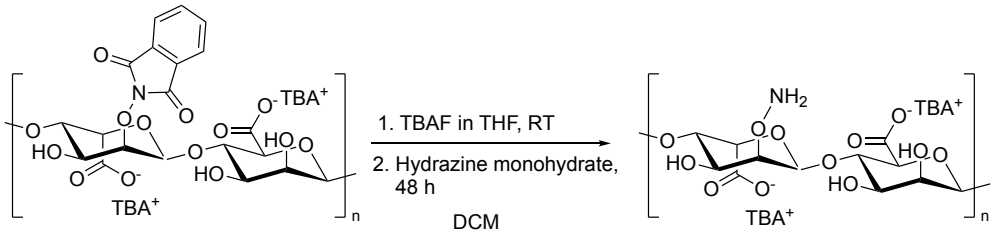

5 **6**

TBA-Alg-*phthal* **5** (0.59 g)was dissolved in a solution of TBAF in THF (1 M, 25 mL), and then added into DCM (CH_2Cl_2, 75 mL) under stirring.. The solution was purged with N_2 gas and hydrazine monohydrate (1.3 mL, 26.8 mmol) was slowly added. The mixture was stirred at room temperature for 48 h. After concentration under vacuum, the residue **6** was used directly in the next step without purification.

Lab book reference: **AMRR011**

Synthesis of Alginate-Alkoxyamine (Alg-AA) 7

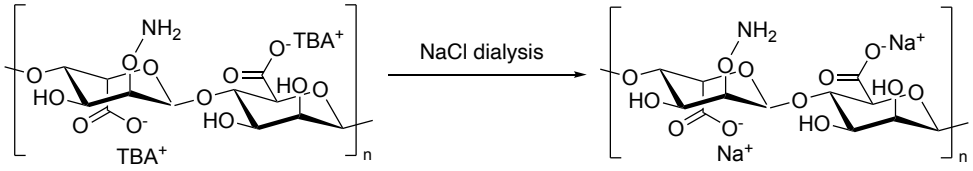

6 **7**

NaAlg-AA **7** was obtained after a 48 h dialysis of TBA-Alg-AA against NaCl saturated water using a 10k MWCO cellulose membrane for two days, followed by a dialysis against DI H_2O on the same membrane for three days. NaAlg-AA **7** (0.35 g) was obtained with a ~59% yield, after lyophilisation and stored at -20°C.

The NaAlg-AA **7** was characterized using ^{1}H NMR (integrals are relative to the smallest peak). ^{1}H NMR (400 MHz, D_2O): 4.81-4.92 (2.5H, m), 4.42-4.49 (1H, m), 3.98-4.07 (1.5H, m), 3.48-3.95 (20H, m), 2.98-3.09 (1H, m).

Lab book reference: **AMRR013**

4.2.3 Development of a novel route to access an Alginate Alkoxyamine (alg-AA) 3

a. Phthalimide-protected alkoxyamine.

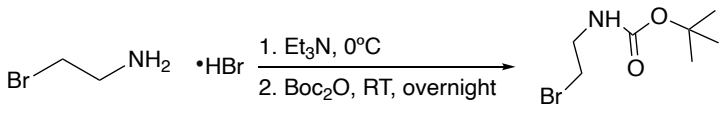

8 **9**

2-Bromoethylamine hydrobromide **8** (4.15 g, 20 mmol) was dissolved in dichloromethane (DCM 38 mL) and the mixture cooled to 0 °C. Next, triethylamine (2 mL, 20 mmol) was added followed by a solution of Boc_2O (4.32 g, 19 mmol) in DCM (5 mL). This mixture was stirred at room temperature for 18 hrs. The organics were then washed with citric acid (5%, 40 mL), water (40 mL) and brine (40 mL), dried over Na_2SO_4, filtered and dried under reduced pressure. 2.49 g, 11 mmol (55% yield) of tert-butyl (2-bromoethyl)carbamate **9** product was obtained. Spectroscopic data were consistent with those previously reported. ^{1}H NMR (400 MHz, $CDCl_3$) δ 4.94 (br s, 1H), 3.53 (t, *J* = 6.0 Hz, 2H), 3.45 (t, *J* = 6.0 Hz, 2H), 1.44 (s, 9H); MS (ESI) *m/z* 246 $(M + Na)^+$.[91]

Lab book reference: **AMRR021**

The second step was performed following the method described in the US Patent US10085999B1,[82] for the synthesis of N-(2-tert-Boc-aminoethoxy)phthalimide.

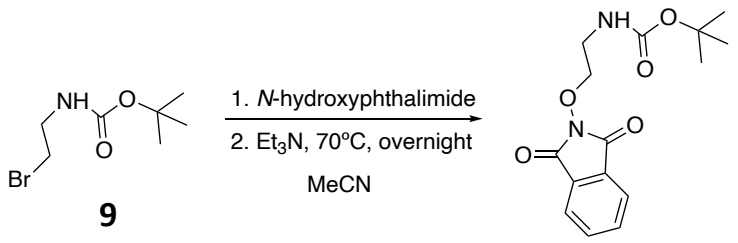

9 **10**

The procedure was adapted from US Patent US10085999B1.[82] Tert-butyl (2-bromoethyl)carbamate **9** (2.49 g, 11.11 mmol) was mixed with *N*-hydroxyphthalimide (1.83 g, 11.15 mmol) in acetonitrile (MeCN, 40 mL). Then, triethylamine (Et_3N 3.8 mL, 26.75 mmol) was added,. The reaction was stirred at 70 °C for 18 h, and after cooling to room temperature was concentrated by evaporation. The residue was then diluted with ethyl acetate (40 mL) and washed with 1 N HCl (40 mL), saturated $NaHCO_3$ (40 mL), and water (40 mL). The organic layer was dried with anhydrous sodium sulfate (Na_2SO4), then filtered and concentrated by evaporation. 1.72 g, 5.6 mmol (50% yield) of N-(2-tert-Boc-aminoethoxy)phthalimide product **10** was obtained as an off white solid. Characterization resulting data were coherent with the reported in literature. ^{1}H NMR (400 MHz, Chloroform-*d*) δ 7.84 (dd, *J* = 5.3, 2.3 Hz, 2H), 7.77 (dd, *J* = 5.3, 2.3 Hz, 2H), 5.65 (br s, 1H), 4.25 (t, *J* = 5.0 Hz, 2H), 3.44 (4, *J* = 5.0 Hz, 2H), 1.46 (s, 9H); MS (ESI) *m/z* 307 $(M + H)^+$; MS (ESI) *m/z* 329 $(M + Na)^+$.[82]

Lab book reference: **AMRR023**

The last step was performed using the method described in the European Patent EP3318567A1,[83] and the amine of interest was obtained.

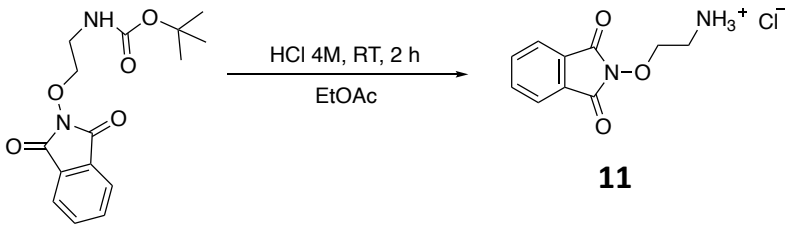

10 **11**

N-(2-Boc-aminoethoxy)phthalimide **10 (**1.72 g, 5.62 mmol) was dissolved in ethyl acetate (EtOAc 14 mL), and a solution of HCl in ethyl acetate (4 M, 1.7 mL) was added. The mixture was stirred at room temperature for 2 h. During this time a white solid formed which was collected and dried under reduced pressure by vacuum filtration. 0.68 g (3.32 mmol, 59% yield) of product **11** was obtained. The results correspond the previously reported. ^{1}H NMR (400 MHz, DMSO-d_6) δ 8.22 (br s, 3H), 7.87-7.91 (m, 4H), 4.36 (t, *J* = 5.5 Hz, 2H), 3.18 (t, *J* = 5.5 Hz 2H); MS (ESI) *m/z* 207 $(M + H)^+$. MS (ESI) *m/z* 229 $(M + Na)^+$.[83]

Lab book reference: **AMRR026**

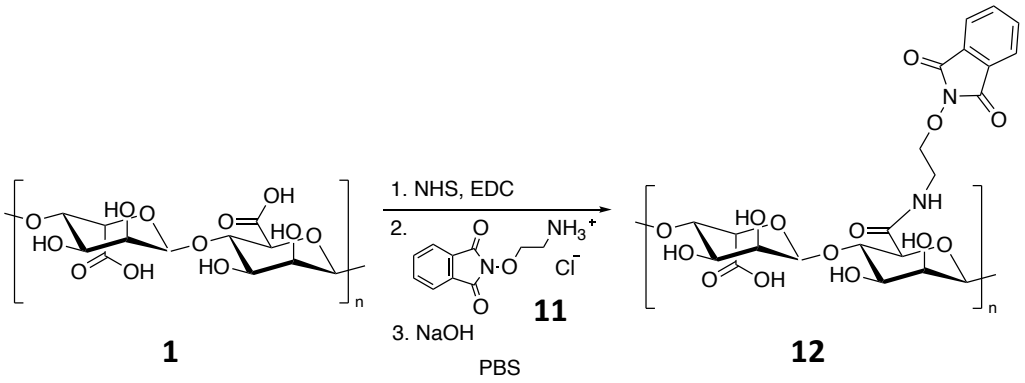

1 **11** **12**

i. First experiment

Sodium Alginate **1** (0.3 g) was added to PBS (50 mL containing 0.3 M NaCl) and stirred for 3 h. After the alginate was dissolved, EDC (0.19 g, 1.22 mmol) was added, followed by NHS (0.06 g, 0.52 mmol) and stirred for 1.5 h. Then, the amine **11** (0.09 g, 0.44 mmol) was added at a 1:8 ratio

of amine to alginate monomers. The solution was stirred overnight, followed by a dialysis against DI H_2O (10 KDa MWCO cellulose membrane) for 2 days. The product **12a** was freeze dried and 0.47 g of coupled alginate were obtained and stored at -20 °C.

Lab book reference: **AMRR033**

ii. Second experiment[85]

Alginate **1** (50 mg) was dissolved in DI H2O (5 mL). Next, NHS (15 mg, 0.13 mmol) and PBS (2 mL) were added. Then the amine **11** (6 mg, 0.03 mmol) was added at a 1:8 ratio of amine to alginate monomers and was stirred for 10 min. EDC (57 mg, 0.37 mmol) was then added and the solution was stirred for 25 min. Then, NaOH (6 M, 55 µL) was added and the solution was purified by dialysis against DI H_2O (10 KDa MWCO membrane) for 4 days changing the water 3 times per day and adding NaOH (6 M, 10 µL) and NaCl (4.26 M, 400 µL) twice a day for the first 3 days. Approximately 3 mL of the remaining solution was filtered using a 0.45 µm membrane and approximately 6 mL was not filtered. The solutions were freeze dried and stored at -20 °C. 12 mg of unfiltered and 5 mg of filtered products **12b** were obtained, with no noticeable differences.

Lab book reference: **AMRR039**

iii. Third experiment[85]

The coupling of alginate was repeated as described in the second trial above, at 6 different ratios of amine to alginate (2:5, 1:4, 1:8, 1:16, 1:32, 1:96) at a 500 mg scale of alginate. 10% of the resulting reactions were purified by dialysis as described above, and 90% was used in the subsequent step The total product **12c** of the dialyzed samples with

coupled alginate was: 29 mg of sample 1, 21 mg of sample 2, 27 mg of sample 3, 17 mg of sample 4, 17 mg of sample 5, and 37 mg of sample 6.

The new Alg-AA coupled to the phthalimide **12c** was characterized using ^{1}H NMR (integrals are relative to the smallest peak) and DOSY NMR. ^{1}H NMR (400 MHz, D_2O): 7.50-7.59 (1H, m), 7.29-7.47 (3H, m), 3.39-4.18 (58H, m).

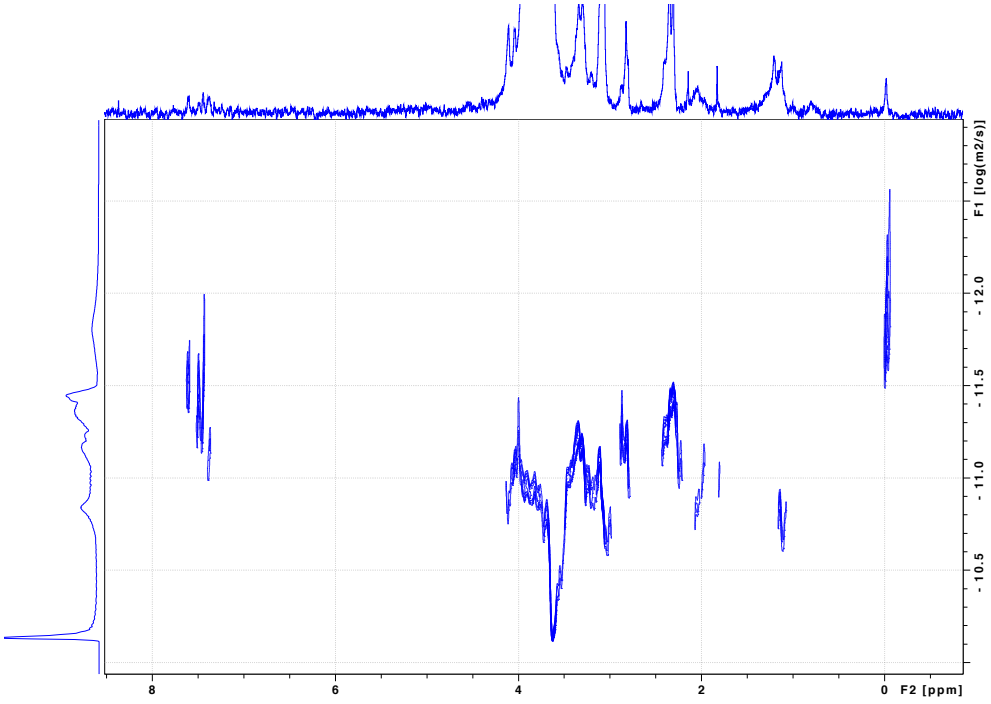

Fig.36. DOSY NMR Spectra of alginate and Na-alg-AA **12c** at 1:96 coupling ratio.

DOSY NMR (Fig. 36) was performed using the pulse program ledbpgppr2s, which uses water suppression, with the parameters: sw 13.7 ppm x 10 ppm, TD 16k x 8, diffusion time **Δ** D20 = 0.15s, diffusion gradient length **δ** p30 = 1ms.

Lab book reference: **AMRR045**

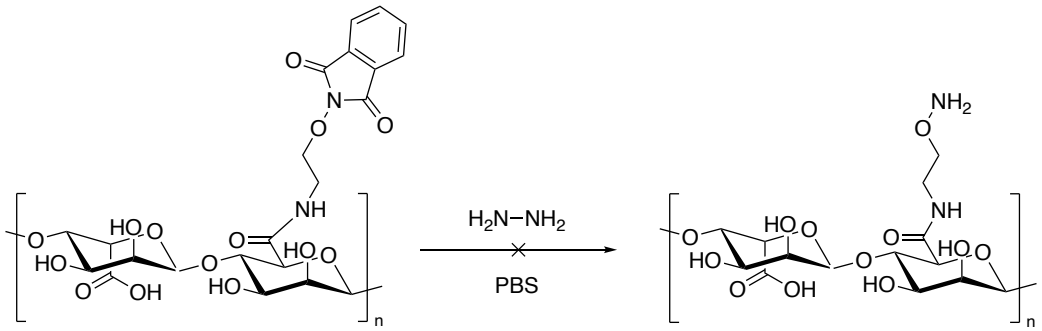

12 **3a**

Hydrazine monohydrate (1.3 mL, 26.8 mmol) was added to solutions of functionalised alginate (63 mL) and stirred for 72 h. The resulting solutions were purified by dialysis against tap water (10 KDa MWCO membrane) for 3 days, and the remaining solutions were freeze dried and stored at -20 °C.

The new Alg-AA coupled to the phthalimide amine and deprotected **3a** was characterized using ^{1}H NMR.

Lab book reference: **AMRR048**

b. Boc-protected alkoxyamine.

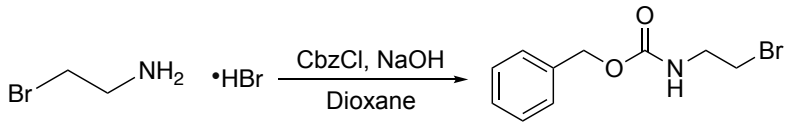

8 **13**

F

2-Bromoethylamine hydrobromide **8** (1.20 g, 5.86 mmol) was dissolved in dioxane (6 mL) at 4 °C. Next, sodium hydroxide (1 M, 11.72 mL, 11.72 mmol) was added. Then benzyl chloroformate (0.84 mL, 5.9 mmol) was added dropwise and stirred at 0 °C for 30 min and then for 18 h at RT. The mixture was then diluted with diethyl ether (Et_2O, 35 mL) an the organics were washed with DI H_2O (7.5 mL dried with anhydrous magnesium sulfate ($MgSO_4$), filtered and evaporated to dryness to

obtain a colourless oil of product **13** (1.64 g, 6.35 mmol, the compound was not fully dry). Characterization corresponds to the reported in literature. ^{1}H NMR (400 MHz, $CDCl_3$): δ 7.32-7.38 (m, 5H), 5.12-5.36 (m, 3H), 3.60 (t, *J* = 5.9 Hz, 2H), 3.47 (t, *J* = 5.9 Hz, 2H).[92]

Lab book reference: **AMRR054**

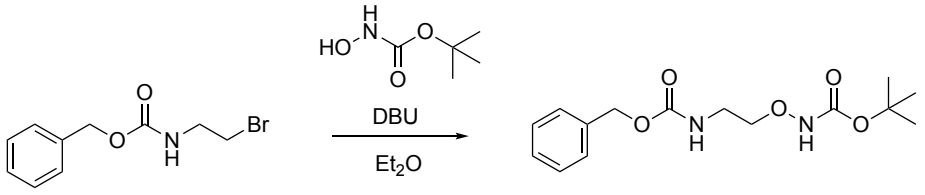

13 **14**

N-Boc-hydroxylamine (0.72 g, 5.41 mmol) was dissolved in a mixture of Et_2O (3 mL) and 1,8-diazabicyclo(5.4.0)undec-7-ene (DBU 0.87 mL). **13** (1 g, 3.87 mmol) was added, and the mixture stirred overnight. The mixture was diluted with Et_2O (80 mL) and the organics washed with DI H_2O (60 mL), $KHSO_4$ (0.1 M, 80 mL), and NaOH (0.1 M, 5 x 20 mL), dried with Na_2SO_4, filtered and concentrated under vacuum. The residue was purified by flash column chromatography eluting with 15-50% EtOAc: Petroleum ether. The pure fractions were combined and the solvent was removed under reduced pressure to give **14** obtaining a transparent oil (0.2 g, 0.64 mmol, 11.8% yield). Resulting data were consistent to previously reported.[92] ^{1}H NMR (400 MHz, $CDCl_3$): δ 7.28-7.37 (m, 5H), 5.74 (br s, 1H), 5.11 (s, 2H), 5.12-5.36 (m, 3H), 3.86 (t, *J* = 5.9 Hz, 2H), 3.43 (t, *J* = 5.9 Hz, 2H), 1.46 (s, 9H); MS (ESI) *m/z* 333 $(M + Na)^+$; MS (ESI) *m/z* 349 $(M + K)^+$.[92]

Lab book reference: **AMRR056**

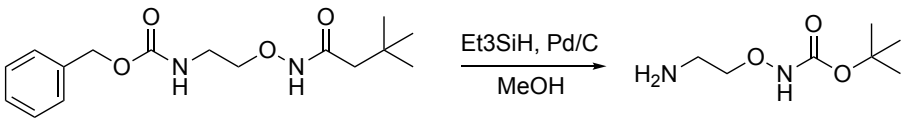

14 **15**

Compound **14 (**0.2 g, 0.64 mmol) was dissolved in methanol (MeOH 3.7 mL). Chloroform (CH_3Cl_3 59 µL) was added. The solution was purged with Argon (Ar) gas and palladium on carbon (Pd/C 5%, ~0.5 g) was then added, Triethylsilane (~1 mL) was added dropwise, and the solution was stirred for 1 h. Then, the solution was filtered through Celite ($CaCO_3$) to remove the Pd/C, keeping the Pd/C phase moist. The filtrate was evaporated to dryness, resulting in the product **15** (0.12 g, 0.68 mmol, the compound was impure). Spectroscopic data was consistent with literature. ^{1}H NMR (400 MHz, $CDCl_3$): δ 4.11-4.20 (m, 2H), 3.25-3.32 (m, 2H), 1.47 (s, 9H).[92]

Lab book reference: **AMRR062**

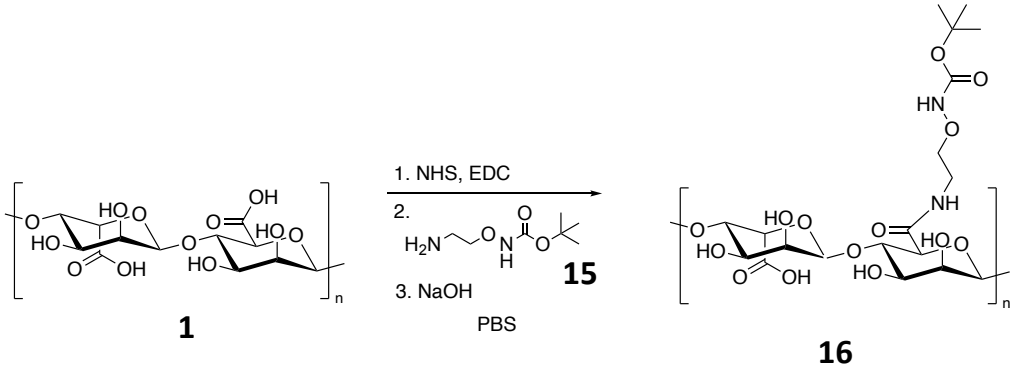

NHS (0.09 g, 0.78 mmol) was added to a solution of Sodium Alginate **1** (40 mL, 1% w/v in DI H_2O). The amine **15** (120 mg, 0.7 mmol) and PBS (12 mL) were added and the mixture stirred for 10 min. EDC (0.34 g, 2.19 mmol) was then added and the solution was stirred for 25 min. Then, NaOH (6 M, 33 µL) was added and stirred for 10 min. The solution was then purified by dialysis against DI H_2O (10 KDa MWCO membrane), and the remaining solution lyophilized giving 0.35 g of **16**, and stored at -20 °C. These were characterised by ^{1}H NMR and DOSY NMR.

DOSY NMR (Fig. 37) was performed using the pulse program ledbpgppr2s, which uses water suppression, with the parameters: sw 13.7 ppm x 10 ppm, TD 16k x 8, diffusion time **Δ** D20 = 0.25s, diffusion gradient length **δ** p30 = 2.5ms.

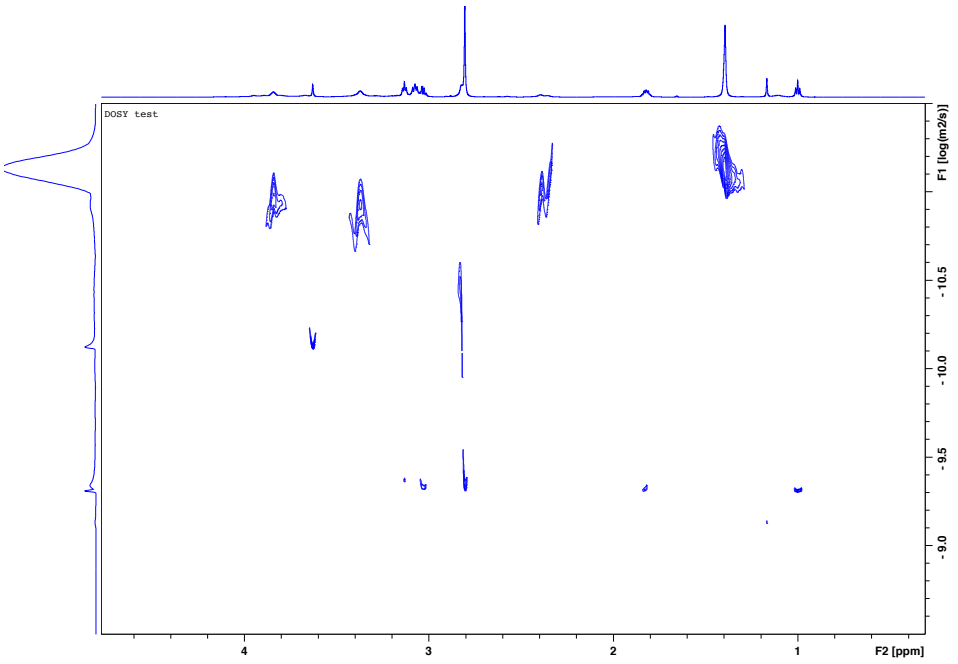

Fig. 37. DOSY NMR Spectra of alginate and coupled Alg-AA **16**.

Lab book reference: **AMRR064**

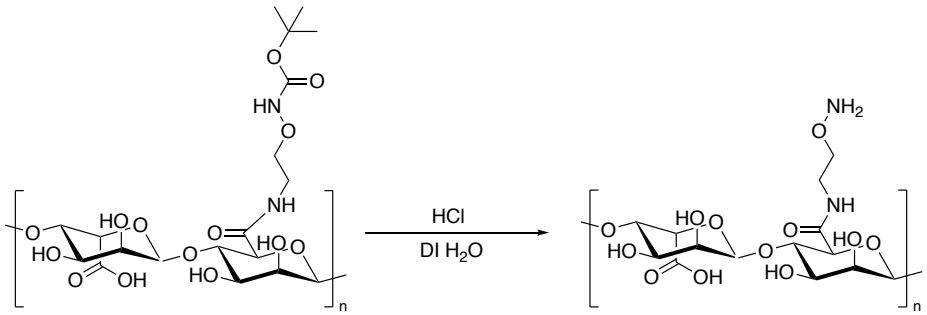

16 **3b**

Coupled alginate **16** (0.1 g) was suspended in DI H_2O (6 mL), . Hydrogen chloride (HCl 1 M, 6 mL) was added and the mixture stirred for 1 h. The resulting solution was purified by dialysis against DI H_2O (10 KDa MWCO membrane) for 3 days, and the remaining solution was freeze dried and stored at -20 °C. Alg- AA **3b** (78 mg) was obtained. This was repeated at a 1:4 ratio, and alg-AA **3b** (165 mg) were obtained, characterised by ^{1}H NMR (integrals are relative to the smallest peak) and stored at -20 °C.

^{1}H NMR (400 MHz, D_2O): 3.56-4.17 (7H, m), 3.28-3.44 (1H, m), 2.73-2.81 (1H, m), 1.31-1.37 (1H, s).

Lab book reference: **AMRR066**, **AMRR091**, **AMRR094**

4.3 Alginate Hydrogels

4.3.1 Ionically Crosslinked Alginate Hydrogels

Stock solutions

Standard concentrations of alginate and calcium solutions were used to make the ionically crosslinked alginate hydrogels, following procedures found in literature. Stock solutions of alginate **1** (1% w/v, 0.4 g) in DI H_2O (40 mL), dispersed calcium sulfate ($CaSO_4$, 16% w/v, 6.6 g, 48.48 mmol) in DI H_2O (40 mL), and calcium chloride dihydrate ($CaCl_2{\cdot}2H_2O$ 0.45 M, 2.65 g, 18.03 mmol) in DI H_2O (40 mL) were prepared according to the previously reported procedures and stored at room temperature.[87,88]

Lab book reference: **AMRR017**, **AMRR019**, **AMRR029**, **AMRR038**, **AMRR051**

Hydrogel formation addition studies

A polystyrene 96-well plate was used as a mould for the gels. Each well had a volume of 500 µL. $CaSO_4$ stock solution was added to each well (100 µL) , and the amount of the alginate solution varied from 50 µL to 200 µL. The gels were left for ~2 h on average. Hydrogels were prepared in different alginate to calcium ratios and using different addition methods, shown in Figure 38.

Lab book reference: **AMRR017**

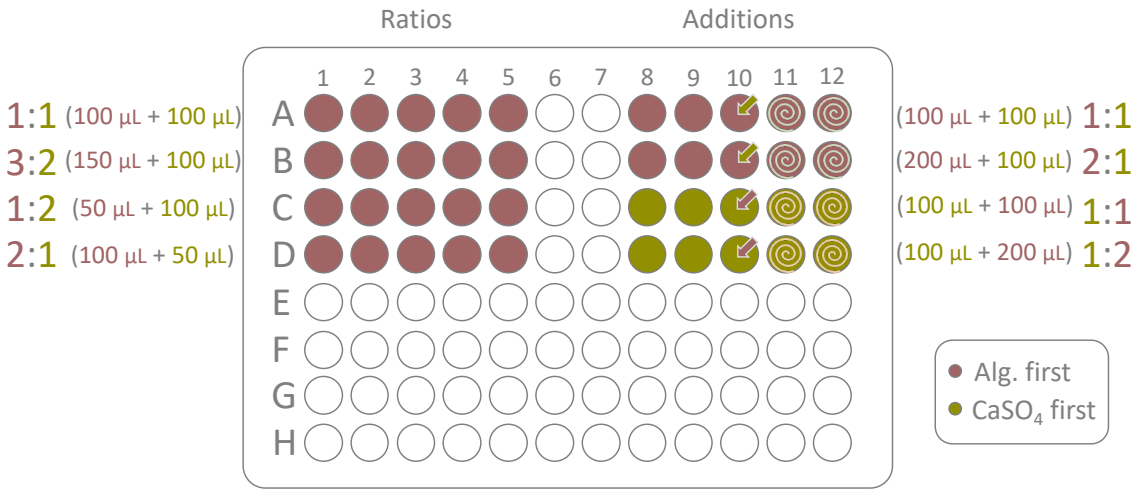

Fig. 38. Organization of the plates. In the maroon coloured wells, alginate was added first and $CaSO_4$ was added next. In the dark wood-green coloured wells, the order of addition was the opposite. Hydrogels in columns 1-5 had a variation of ratios, and in the columns 8-12 the addition methods were varied. The arrow in column 10 represents the addition inside of the solution, and the spirals on columns 11-12 represent mixing motions.

Next, in a polystyrene 96-well plate, 3 hydrogels were made using a $CaCl_2$ stock solution in DI H_2O (5% w/v) as a crosslinker. Each well had a volume of ~500 µL. The hydrogels were prepared at a 1:1 alginate to crosslinker ratio. The alginate solution (120 µL) was added into the wells, and $CaCl_2$ solution (120 µL) was pipetted on top. For the first hydrogel (well A1, Fig. 39, A), the calcium solution was added dropwise on top. For the second hydrogel (well A3, Fig. 39, B), $CaCl_2$ solution was added to the side of the well with a slow and constant flow. Finally, for the third hydrogel (well A5, Fig. 39, C), the calcium solution was added fast on top.

Lab book reference: **AMRR031**

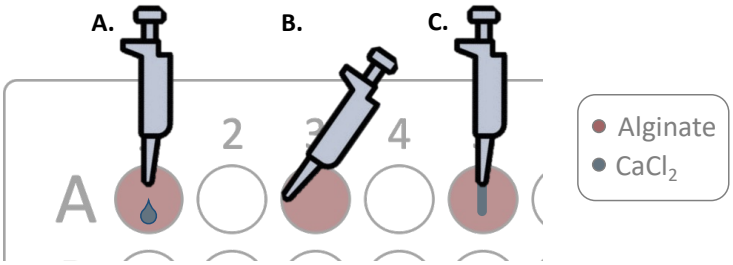

Fig. 39. Types of addition of $CaCl_2$ solution on top of Alginate solution: **A.** dropwise, **B.** constant flow on the side, **C.** quickly added on top.

Moulds and materials to shape the hydrogels

96-well plates of different materials with 8 mm diameter cylindric moulds were used to form the hydrogels. Initially, a 96-well plate (polystyrene) was used, followed by a 96-well bottomless plate and using unattached aluminium foil base, a polystyrene base, a glass base, and silicon base with and without uniformly distributed weight on top (380 - 400 g). Next, a 96-well bottomless plate of Polytetrafluoroethylene (PTFE) was used on top of silicon and 400 g of weight on top.

36 hydrogels were made in each mould (Fig. 40) using $CaCl_2$ in DI H_2O stock solution as a crosslinker. Each well had a volume of ~450 µL. The hydrogels were prepared at three different alginate to crosslinker ratios. The plate was sectioned in four parts. Two vertical blocks, the left side had an addition of alginate followed by the addition of $CaCl_2$, whereas the right side of the plate had $CaCl_2$ added before and the alginate added on top. Each block had a two blocks, where the top block had a constant volume of alginate of 150 µL per well, and the bottom block had a constant total volume of solution of 300 µL per well. These hydrogels were prepared and left for ~2.5 h.

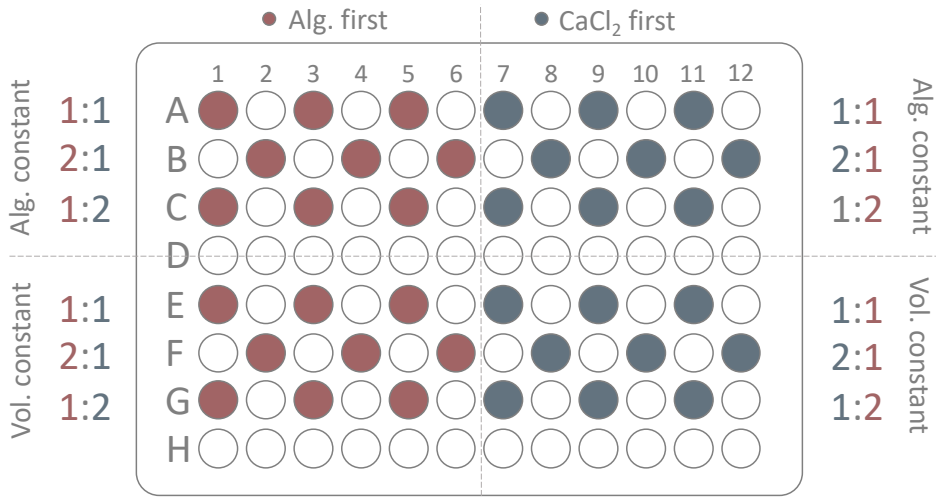

Fig. 40. Organization of the plates. In the maroon coloured wells, alginate was added first and $CaCl_2$ was added next. In the grey coloured wells, the order of addition was the opposite. Rows A-C kept the alginate volume constant (150 µL), and rows E-G kept total volume constant (300 µL).

Lab book reference: **AMRR030**, **AMRR036**, **AMRR043**, **AMRR051**, **AMRR052**

Custom-made silicone moulds were manufactured by the group using a silicone mould making kit, mixing two phases. First, a bioplastic was used to create a negative (1 cm height and 8 mm diameter) by warming it up in warm water (following the product instructions) and once mouldable, it was inserted inside one of the 96-well plate wells and removed before fully solidification (approx. 15 s). Next, the two silicone phases were mixed and added into a glass vial (~2 cm height and 1 cm diameter) until half-filled. Then, the bioplastic negative was inserted carefully in the middle, making sure it was centred. This was demoulded after ~10 h and the bioplastic was reused. A hydrogel was made using the silicone mould by adding 150 µL of alginate stock solution on top of 150 µL of $CaCl_2$ crosslinker solution.

Lab book reference: **AMRR096**

4.3.2 Novel Oxime Crosslinked Alginate Hydrogels

Ionically crosslinking of components: alg-ald 2 and alg-AA 3b

In 0.5 mL Eppendorfs, alginate-aldehyde **2** (500 μg) of varying degree of oxidation (25%, 50%, or 75%) was dissolved in DI H_2O (50 μL) at a 1% w/v concentration. Alternatively, alginate alkoxyamine **3b** (500 μg) was dissolved in DI H_2O (50 μL) at a 1% w/v concentration. Into each Eppendorf, a $CaSO_4$ stock solution (50 μL, 16% w/v in DI H_2O) was added on top. Observations of the solutions were made after 6 h and 30 h.

The experiment was reproduced using a $CaCl_2$ (5% w/v in DI H_2O) stock solution. The pH was measured for the solutions: pH 4.4 alg-ald 50% DOx **2**, pH 2.7 the alg-AA **3b**, and pH 5.6 $CaCl_2$ solution.

Lab book reference: **AMRR070**

Preparation of novel oxime crosslinked hydrogels In DI H_2O

Alginate-aldehyde **2** at a 50% DOx (30 μg) was dissolved in DI H_2O (3 mL), and alginate-alkoxyamine **3b** (30 μg) was dissolved in DI H_2O (3 mL), to create 1% w/v solutions.

In a polystyrene 96-well plate, the alg-ald solution (A: 200 μL; B: 100 μL; C: 100 μL) was added on top of alg-AA solution (A: 100 μL, B: 100 μL, C: 200 μL) at three different ratios (A: 1:2; B: 1:1; and C: 2:1) and in replicates, and left to stand at room temperature. This was repeated using a hollow polystyrene 96-well plate on top of a silicone base with a ~550 g weight uniformly distributed on top. Observations were made after 4 h and 24 h.

Lab book reference: **AMRR068**

Reproducing the oxime crosslinked hydrogel previously reported in the Roh Group

Alginate-aldehyde 50% DOx **2** (5 mg) and Alg-AA **7** (5 mg) solutions were made by dissolving each component in separate flasks in PBS, or pH 6 or pH 8 phosphate buffers (500 μL) at a

1% w/v concentration. The hydrogels were prepared in a 2 mL glass vial by mixing 500 µL of each solution. The gelation of the three hydrogels was monitored for 14 days.

Lab book reference: **AMRR102**

Preparation of novel oxime crosslinked hydrogels In buffer

Alginate-aldehyde **2** (50% Dox, 5 mg) and Alg-AA **3b** (5 mg) were dissolved in separate flasks in PBS, or pH 6 or pH 8 phosphate buffers (500 µL) at a 1% w/v concentration. Oxime crosslinked alginate hydrogels were prepared by mixing alg-ald **2** (500 µL) and alg-AA **3b** (500 µL) solutions in 2 mL glass vials. As a control, 2 ionically crosslinked alginate hydrogels were prepared in 2 mL glass vials by adding alginate stock solution (1 mL, 1% w/v in DI H_2O) and adding $CaCl_2$ stock solution (1 mL, 5% w/v in DI H_2O) slowly to the side of the vial. Observations were made during a period of 14 days.

Lab book reference: **AMRR102**

Rheological studies of novel oxime crosslinked hydrogels

Gels were prepared as described above in triplicates (Fig. 41).

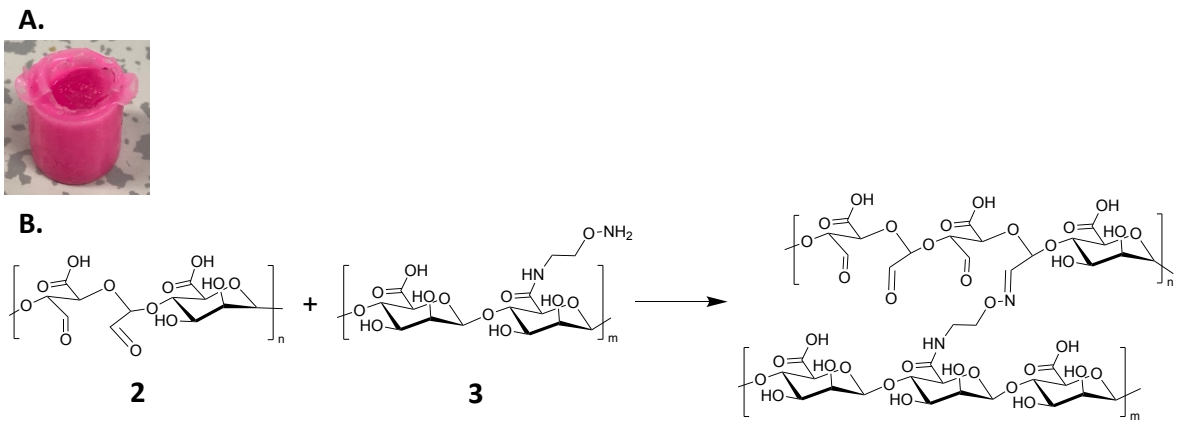

Fig. 41. Oxime crosslinked hydrogel preparation. **A**. Hydrogels prepared in custom made silicone moulds. **B**. Mechanism of the oxime crosslinking between the alginate-aldehyde **2** and the alginate-alkoxyamine **3b**.

After ~20 h, rheological experiments were performed. First, an amplitude sweep was performed at 25 °C, with a shear strain of 0.1-100%, 1 Hz frequency and 50 samples per decade. Next, a frequency sweep was performed at 25 °C, 0.1% shear strain, 0.1-100 Hz frequency, and 50 samples per decade. The measurements were made in triplicates, but a representative example of each was used as example. Data are presented in Figures 42-44.

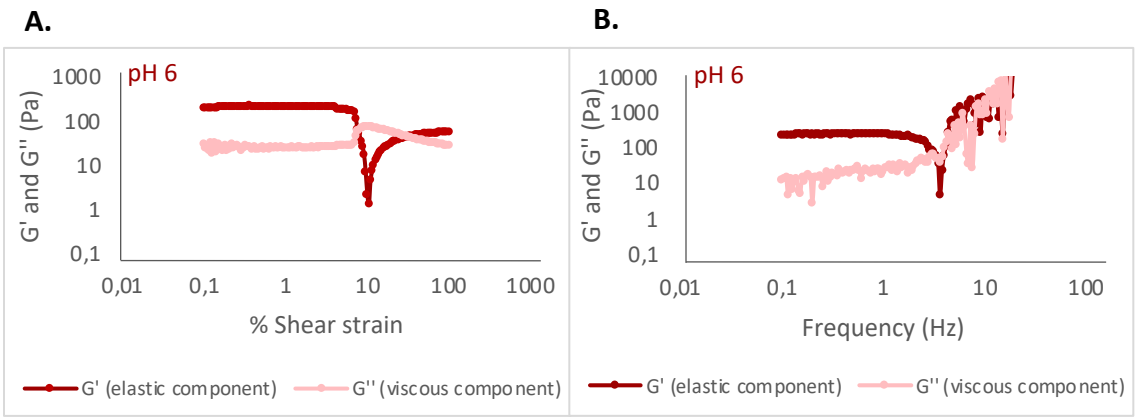

Fig. 42. Elastic (G', in dark red) and viscous (G'', in light red) moduli of oxime crosslinked hydrogels (1% w/v at 1:1 ratio) in pH 6 buffer, with increasing shear strain (**A**) and frequency (**B**).

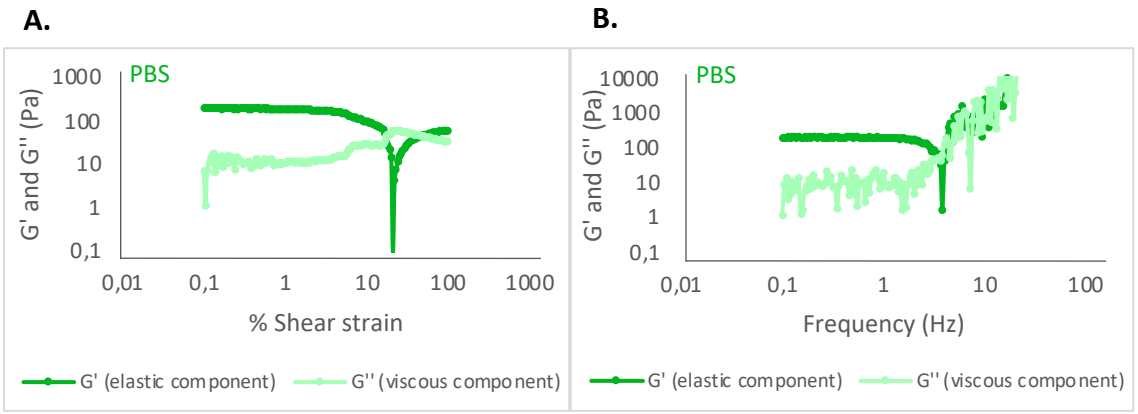

Fig. 43. Elastic (G', in dark green) and viscous (G'', in light green) moduli of oxime crosslinked hydrogels (1% w/v at 1:1 ratio) in PBS, with increasing shear strain (**A**) and frequency (**B**).

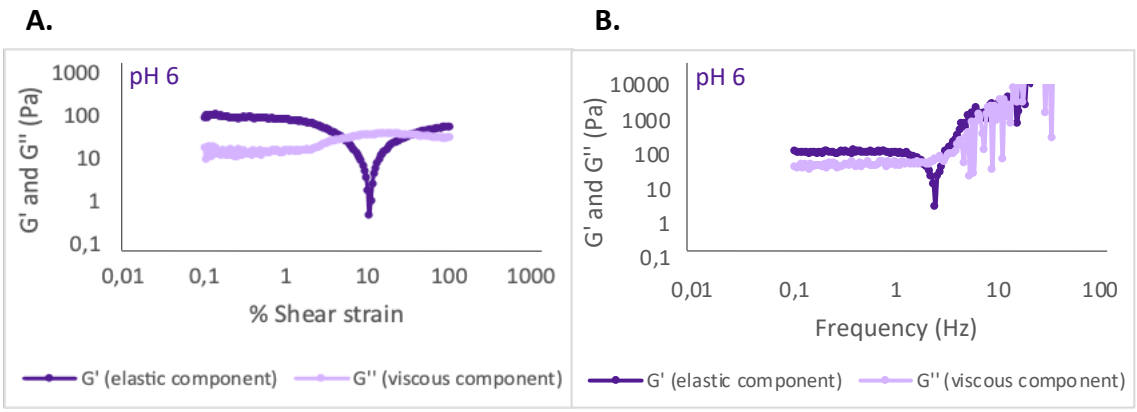

Fig. 44. Elastic (G', in dark purple) and viscous (G'', in light purple) moduli of oxime crosslinked hydrogels (1% w/v at 1:1 ratio) in pH 8 buffer, with increasing shear strain (**A**) and frequency (**B**).

Lab book reference: **AMRR102**

5. References

[1] Hau J. Animal models for human diseases: an overview. Sourcebook of models for biomedical research. 2008:3-8.

[2] Hau J, Van Hoosier GL. Animal models. Handbook of Laboratory Animal Science: Animal Models. 2002:1-9.

[3] Russell WM, Burch RL. The principles of humane experimental technique. Methuen; 1959.

[4] Balls M. It's time to include harm to humans in harm–benefit analysis—But how to do it, that is the question. Alternatives to Laboratory Animals. 2021;49(5):182-96.

[5] Hollands C. The animals (scientific procedures) act 1986. Lancet (London, England). 1986;2(8497):32-3.

[6] Akhtar A. The flaws and human harms of animal experimentation. Cambridge Quarterly of Healthcare Ethics. 2015;24(4):407-19.

[7] Kola I, Landis J. Can the pharmaceutical industry reduce attrition rates?. Nature reviews Drug discovery. 2004;3(8):711-6.

[8] Garner JP. The significance of meaning: why do over 90% of behavioral neuroscience results fail to translate to humans, and what can we do to fix it?. Ilar Journal. 2014;55(3):438-56.

[9] Moreno L, Pearson AD. How can attrition rates be reduced in cancer drug discovery?. Expert opinion on drug discovery. 2013;8(4):363-8.

[10] Van Norman GA. Limitations of animal studies for predicting toxicity in clinical trials: is it time to rethink our current approach?. JACC: Basic to Translational Science. 2019;4(7):845-54.

[11] Sun D, Gao W, Hu H, Zhou S. Why 90% of clinical drug development fails and how to improve it?. Acta Pharmaceutica Sinica B. 2022;12(7):3049-62.

[12] Van der Worp HB, Howells DW, Sena ES, Porritt MJ, Rewell S, O'Collins V, Macleod MR. Can animal models of disease reliably inform human studies?. PLoS medicine. 2010 Mar;7(3):e1000245.

[13] Leenaars CH, Kouwenaar C, Stafleu FR, Bleich A, Ritskes-Hoitinga M, De Vries R, Meijboom FL. Animal to human translation: a systematic scoping review of reported concordance rates. Journal of translational medicine. 2019;17(1):1-22.

[14] Harrison RK. Phase II and phase III failures: 2013–2015. Nat Rev Drug Discov. 2016;15(12):817-8.

[15] Bottini AA, Hartung T. Food for thought… on the economics of animal testing. ALTEX-Alternatives to animal experimentation. 2009;26(1):3-16

[16] Esmon CT. Why do animal models (sometimes) fail to mimic human sepsis?. Critical care medicine. 2004;32(5):S219-22.

[17] Weill A, Païta M, Tuppin P, Fagot JP, Neumann A, Simon D, Ricordeau P, Montastruc JL, Allemand H. Benfluorex and valvular heart disease: a cohort study of a million people with diabetes mellitus. Pharmacoepidemiology and drug safety. 2010;19(12):1256-62.

[18] Ribera R. Valvular heart disease associated with benfluorex. Revista Española de Cardiología. 2003;56(2):215-6.

[19] Le Ven F, Tribouilloy C, Habib G, Gueffet JP, Marechaux S, Eicher JC, Blanchard-Lemoine B, Rousseau J, Henon P, Jobic Y, Etienne Y. Valvular heart disease associated with benfluorex therapy: results from the French multicentre registry. European Journal of Echocardiography. 2011;12(4):265-71.

[20] Kovalkovičová N, Šutiaková I, Pistl J, Šutiak V. Some food toxic for pets. Interdisciplinary toxicology. 2009;2(3):169.

[21] Araújo RG, Rodriguez-Jasso RM, Ruiz HA, Pintado MM, Aguilar CN. Avocado by-products: Nutritional and functional properties. Trends in Food Science & Technology. 2018;80:51-60.

[22] Franco R, Oñatibia-Astibia A, Martínez-Pinilla E. Health benefits of methylxanthines in cacao and chocolate. Nutrients. 2013;5(10):4159-73.

[23] Arck PC. When 3 Rs meet a forth R: Replacement, reduction and refinement of animals in research on reproduction. Journal of Reproductive Immunology. 2019;132:54-9.

[24] Home Office UK. Annual statistics of scientific procedures on living animals Great Britain 2021.

[25] Balls M. It's time to reconsider the principles of humane experimental technique. Alternatives to Laboratory Animals. 2020;48(1):40-6.

[26] Goldberg AM. The principles of humane experimental technique: is it relevant today?. ALTEX-Alternatives to animal experimentation. 2010;27(2):149-51.

[27] Perry P. The ethics of animal research: a UK perspective. ILAR journal. 2007;48(1):42-6.

[28] Ericsson AC, Crim MJ, Franklin CL. A brief history of animal modeling. Missouri medicine. 2013;110(3):201.

[29] Woolston C. Discrimination still plagues science. Nature. 2021;600(7887):177-9.

[30] Analytics C. Highly Cited Researchers. Clarivate Analytics. 2022.

[31] Tabak LA, Collins FS. Weaving a richer tapestry in biomedical science. Science. 2011;333(6045):940-1.

[32] Wanelik KM, Griffin JS, Head ML, Ingleby FC, Lewis Z. Breaking barriers? Ethnicity and socioeconomic background impact on early career progression in the fields of ecology and evolution. Ecology and Evolution. 2020;10(14):6870-80.

[33] Van Norman GA. Limitations of animal studies for predicting toxicity in clinical trials: Part 2: Potential alternatives to the use of animals in preclinical trials. Basic to Translational Science. 2020;5(4):387-97.

[34] Sánchez-Morán H, Ahmadi A, Vogler B, Roh KH. Oxime cross-linked alginate hydrogels with tunable stress relaxation. Biomacromolecules. 2019;20(12):4419-29.

[35] Samanta S, Kim S, Saito T, Sokolov AP. Polymers with dynamic bonds: adaptive functional materials for a sustainable future. The Journal of Physical Chemistry B. 2021;125(33):9389-401.

[36] Muir VG, Burdick JA. Chemically modified biopolymers for the formation of biomedical hydrogels. Chemical reviews. 2020;121(18):10908-49.

[37] Grover GN, Lam J, Nguyen TH, Segura T, Maynard HD. Biocompatible hydrogels by oxime click chemistry. Biomacromolecules. 2012;13(10):3013-7.

[38] Nadgorny M, Xiao Z, Connal LA. 2D and 3D-printing of self-healing gels: design and extrusion of self-rolling objects. Molecular Systems Design & Engineering. 2017;2(3):283-92.

[39] Holzapfel GA. Biomechanics of soft tissue. The handbook of materials behavior models. 2001;3(1):1049-63.

[40] Theodorakou C, Farquharson MJ. Human soft tissue analysis using x-ray or gamma-ray techniques. Physics in Medicine & Biology. 2008;53(11):R111.

[41] Tang S, Richardson BM, Anseth KS. Dynamic covalent hydrogels as biomaterials to mimic the viscoelasticity of soft tissues. Progress in Materials Science. 2021;120:100738.

[42] Bhattacharya A, Devaraj NK. Tailoring the shape and size of artificial cells. ACS nano. 2019;13(7):7396-401.

[43] Jackson SJ, Prior H, Holmes A. The use of human tissue in safety assessment. Journal of Pharmacological and Toxicological Methods. 2018;93:29-34.

[44] Loh QL, Choong C. Three-Dimensional Scaffolds for Tissue Engineering Applications: Role of Porosity and Pore Size. Tissue Engineering Part B: Reviews. 2013;19(6):485–502.

[45] Sarquis J. Colloidal systems. Journal of Chemical Education. 1980;57(8):602.

[46] Bertsch P, Andrée L, Besheli NH, Leeuwenburgh SC. Colloidal hydrogels made of gelatin nanoparticles exhibit fast stress relaxation at strains relevant for cell activity. Acta Biomaterialia. 2022;138:124-32.

[47] Maitra J, Shukla VK. Cross-linking in hydrogels-a review. Am. J. Polym. Sci. 2014;4(2):25-31.

[48] Ahmed EM. Hydrogel: Preparation, characterization, and applications: A review. Journal of advanced research. 2015;6(2):105-21.

[49] Dragan ES. Design and applications of interpenetrating polymer network hydrogels. A review. Chemical Engineering Journal. 2014;243:572-90.

[50] Spicer CD. Hydrogel scaffolds for tissue engineering: The importance of polymer choice. Polymer Chemistry. 2020;11(2):184-219.

[51] Käsdorf BT, Arends F, Lieleg O. Diffusion regulation in the vitreous humor. Biophysical journal. 2015;109(10):2171-81.

[52] Lindberg GC, Longoni A, Lim KS, Rosenberg AJ, Hooper GJ, Gawlitta D, Woodfield TB. Intact vitreous humor as a potential extracellular matrix hydrogel for cartilage tissue engineering applications. Acta biomaterialia. 2019;85:117-30.

[53] Dragan ES. Design and applications of interpenetrating polymer network hydrogels. A review. Chemical Engineering Journal. 2014;243:572-90.

[54] Mantha S, Pillai S, Khayambashi P, Upadhyay A, Zhang Y, Tao O, Pham HM, Tran SD. Smart hydrogels in tissue engineering and regenerative medicine. Materials. 2019;12(20):3323.

[55] Huettner N, Dargaville TR, Forget A. Discovering cell-adhesion peptides in tissue engineering: beyond RGD. Trends in biotechnology. 2018;36(4):372-83.

[56] Davis GE. Affinity of integrins for damaged extracellular matrix: αvβ3 binds to denatured collagen type I through RGD sites. Biochemical and biophysical research communications. 1992;182(3):1025-31.

[57] Keshvardoostchokami M, Majidi SS, Huo P, Ramachandran R, Chen M, Liu B. Electrospun nanofibers of natural and synthetic polymers as artificial extracellular matrix for tissue engineering. Nanomaterials. 2020;11(1):21.

[58] Sell SA, Wolfe PS, Garg K, McCool JM, Rodriguez IA, Bowlin GL. The use of natural polymers in tissue engineering: a focus on electrospun extracellular matrix analogues. Polymers. 2010;2(4):522-53.

[59] Bhatia S, Bhatia S. Natural polymers vs synthetic polymer. Natural Polymer Drug Delivery Systems: Nanoparticles, Plants, and Algae. 2016:95-118.

[60] Kulkarni Vishakha S, Butte Kishor D, Rathod Sudha S. Natural polymers–A comprehensive review. International journal of research in pharmaceutical and biomedical sciences. 2012;3(4):1597-613.

[61] Qin Y. Gel swelling properties of alginate fibers. Journal of applied polymer science. 2004;91(3):1641-5.

[62] Aramwit P. Introduction to biomaterials for wound healing. In Wound healing biomaterials. Woodhead Publishing. 2016;3-38.

[63] Qin Y, Hu H, Luo A. The conversion of calcium alginate fibers into alginic acid fibers and sodium alginate fibers. Journal of applied polymer science. 2006;101(6):4216-21.

[64] Desai RM, Koshy ST, Hilderbrand SA, Mooney DJ, Joshi NS. Versatile click alginate hydrogels crosslinked via tetrazine–norbornene chemistry. Biomaterials. 2015;50:30-7.

[65] Lee P, Rogers MA. Effect of calcium source and exposure-time on basic caviar spherification using sodium alginate. International Journal of Gastronomy and Food Science. 2012;1(2):96-100.

[66] Cai J, Chen X, Wang X, Tan Y, Ye D, Jia Y, Liu P, Yu H. High-water-absorbing calcium alginate fibrous scaffold fabricated by microfluidic spinning for use in chronic wound dressings. RSC advances. 2018;8(69):39463-9.

[67] Taylor DL, in het Panhuis M. Self-healing hydrogels. Advanced Materials. 2016;28(41):9060-93.

[68] Jiang Z, Bhaskaran A, Aitken HM, Shackleford IC, Connal LA. Using synergistic multiple dynamic bonds to construct polymers with engineered properties. Macromolecular rapid communications. 2019;40(10):1900038.

[69] Jin Y, Yu C, Denman RJ, Zhang W. Recent advances in dynamic covalent chemistry. Chemical Society Reviews. 2013;42(16):6634-54.

[70] Rosales AM, Vega SL, DelRio FW, Burdick JA, Anseth KS. Hydrogels with reversible mechanics to probe dynamic cell microenvironments. Angewandte Chemie International Edition. 2017;56(40):12132-6.

[71] Dirksen A, Hackeng TM, Dawson PE. Nucleophilic catalysis of oxime ligation. Angewandte Chemie. 2006;118(45):7743-6.

[72] Sims MB, Patel KY, Bhatta M, Mukherjee S, Sumerlin BS. Harnessing imine diversity to tune hyperbranched polymer degradation. Macromolecules. 2018;51(2):356-63.

[73] Rizwan M, Baker AE, Shoichet MS. Designing hydrogels for 3D cell culture using dynamic covalent crosslinking. Advanced Healthcare Materials. 2021;10(12):2100234.

[74] Morgan FL, Fernández-Pérez J, Moroni L, Baker MB. Tuning Hydrogels by Mixing Dynamic Cross-Linkers: Enabling Cell-Instructive Hydrogels and Advanced Bioinks. Advanced Healthcare Materials. 2022;11(1):2101576.

[75] Hafeez S, Ooi HW, Morgan FL, Mota C, Dettin M, Van Blitterswijk C, Moroni L, Baker MB. Viscoelastic oxidized alginates with reversible imine type crosslinks: self-healing, injectable, and bioprintable hydrogels. Gels. 2018;4(4):85.

[76] Mohabatpour F, Yazdanpanah Z, Papagerakis S, Chen X, Papagerakis P. Self-crosslinkable oxidized alginate-carboxymethyl chitosan hydrogels as an injectable cell carrier for in vitro dental enamel regeneration. Journal of Functional Biomaterials. 2022;13(2):71.

[77] Emami Z, Ehsani M, Zandi M, Foudazi R. Controlling alginate oxidation conditions for making alginate-gelatin hydrogels. Carbohydrate polymers. 2018;198:509-17.

[78] Bouhadir KH, Lee KY, Alsberg E, Damm KL, Anderson KW, Mooney DJ. Degradation of partially oxidized alginate and its potential application for tissue engineering. Biotechnology progress. 2001;17(5):945-50.

[79] Reynolds AJ, Kassiou M. Recent advances in the Mitsunobu reaction: modifications and applications to biologically active molecules. Curr. Org. Chem. 2009;13(16):1610-32.

[80] Camp D, Jenkins ID. The use of a phosphine containing a basic group in the Mitsunobu esterification reaction. Australian Journal of Chemistry. 1988;41(12):1835-9.

[81] Itô S, Tsunoda T. New Mitsunobu reagents in the C–C bond formation. Application to natural product synthesis. Pure and applied chemistry. 1999;71(6):1053-7.

[82] Arixa Pharmaceuticals Inc, Beta-lactamase inhibitors and uses thereof. US Patent US10085999B1.

[83] Shionogi and Co Ltd, TRICYCLIC COMPOUND HAVING SULFINYL OR SULFONYL. European Patent EP3318567 (2018) A1.

[84] Fan L, Cao M, Gao S, Wang T, Wu H, Peng M, Zhou X, Nie M. Preparation and characterization of sodium alginate modified with collagen peptides. Carbohydrate polymers. 2013;93(2):380-5.

[85] Gattás-Asfura KM, Stabler CL. Chemoselective cross-linking and functionalization of alginate via Staudinger ligation. Biomacromolecules. 2009;10(11):3122-9.

[86] Niemeier JK, Kjell DP. Hydrazine and aqueous hydrazine solutions: evaluating safety in chemical processes. Organic Process Research & Development. 2013;17(12):1580-90.

[87] Kuo CK, Ma PX. Ionically crosslinked alginate hydrogels as scaffolds for tissue engineering: Part 1. Structure, gelation rate and mechanical properties. Biomaterials. 2001;22(6):511-21.

[88] Jang J, Seol YJ, Kim HJ, Kundu J, Kim SW, Cho DW. Effects of alginate hydrogel cross-linking density on mechanical and biological behaviors for tissue engineering. journal of the mechanical behavior of biomedical materials. 2014;37:69-77.

[89] Chan ES, Lee BB, Ravindra P, Poncelet D. Prediction models for shape and size of ca-alginate macrobeads produced through extrusion–dripping method. Journal of colloid and interface science. 2009;338(1):63-72.

[90] Discher DE, Mooney DJ, Zandstra PW. Growth factors, matrices, and forces combine and control stem cells. Science. 2009;324(5935):1673-7.

[91] Borodin O, Shchukin Y, Robertson CC, Richter S, von Delius M. Self-Assembly of Stimuli-Responsive [2] Rotaxanes by Amidinium Exchange. Journal of the American Chemical Society. 2021;143(40):16448-57.

[92] Carrasco MR, Alvarado CI, Dashner ST, Wong AJ, Wong MA. Synthesis of aminooxy and N-alkylaminooxy amines for use in bioconjugation. The Journal of Organic Chemistry. 2010;75(16):5757-9.